Heterogeneous Catalytic Synthesis of Methyl Lactate and Lactic Acid from Sugars and Their Derivatives
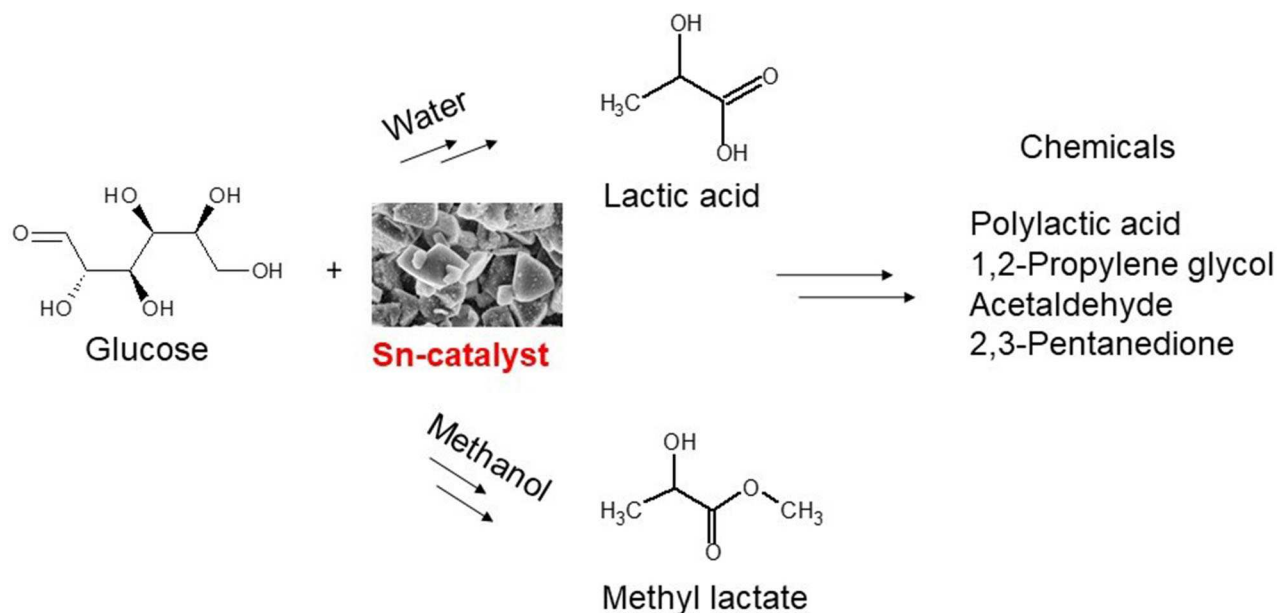
Päivi Mäki-Arvela,[a] Atte Aho,[a] and Dmitry Yu. Murzin*[a]

ChemSusChem

Reviews
doi.org/10.1002/cssc.202001223

**Chemistry
Europe**
European Chemical
Societies Publishing

Recent developments in sugar transformations to methyl lactate and lactic acid are critically summarized. The highest yield of methyl lactate from glucose obtained over Sn(salen)/octylmethyl imidazolium bromide catalyst was 68% at 160 °C whereas the highest yield of lactic acid of 58% was achieved over hierarchical Lewis acidic Sn-Beta catalysts at 200 °C under inert atmosphere. In addition to the desired products also humins are formed in water whereas in methanol alkyl glucosides- and -fructosides as well as acetals were generated, especially in the presence of Brønsted-acidic sites. The main challenges limiting the industrial feasibility of these reactions are incomplete liquid phase mass balance closure, complicated product analysis and a lack of kinetic data. In addition to reporting optimized reaction conditions and catalyst properties also catalyst reuse and regeneration as well as kinetic modelling and continuous operation are summarized.

1. Introduction

Biomass transformation to value-added products has been under intensive research efforts in the recent years.[1–36] The target in biorefinery has been to transfer highly abundant biomass to chemicals and fuels.[37,38] Sugars, such as glucose and xylose, are considered as the key platform chemicals, which can be further valorized to a range of valuable products, including lactic acid or its esters.

The aim of this Review is to elucidate recent developments in transformation of sugars, trioses, sucrose and inulin to lactic acid (LA) and methyl lactate (ML) (Figure 1). In addition to sugars as feedstock, also one-pot production of LA via transformation of hemicellulose and cellulose has been demonstrated using Y^{III} as a catalyst giving a yield of LA up to 66.3%.[39] LA is used as a raw material for polylactic acid, 1,2-propylene glycol, acetaldehyde, and 2,3-pentanedione[36] and its market value in 2014 was 4129 million USD.[40] Other catalytic methods to produce LA are glycerol dehydration[41,42] and fermentation.[43,44] Feasibility of heterogeneously catalysed LA and alkyl lactate industrial production is still under debate. Despite several attempts for direct transformations of sugars to LA and alkyl lactates,[1–35] relatively low yields of LA (58%)[33] and alkyl lactates (68%),[7,18,33] are obtained due to several side reactions,[9,11,18,30,34] originating from too high Brønsted acidity, which is required for the main reaction. Furthermore, the carbon balance in sugar transformation in water is only 80%.[34] The primary product of glucose transformation is fructose, formed via aldose-ketose isomerization (Figure 1b)[13,18] and several additional step are required to produce LA.

In this work the authors collected the data on the yields of alkyl lactates and LA in sugar transformations reported so far (Table 1). A special effort was put on a discussion of catalyst properties, and analysing performance of hierarchical zeolites[3,7,8] and nanosized zeolites[4,13] in comparison with conventional microporous materials. This Review also covers sugar transformation over zeolites and other catalysts.

[a] Prof. P. Mäki-Arvela, Dr. A. Aho, Prof. D. Y. Murzin
Johan Gadolin Process Chemistry Centre, Laboratory of Industrial Chemistry and Reaction Engineering
Åbo Akademi University
Turku/Åbo (Finland)
E-mail: dmurzin@abo.fi

The effect of reaction conditions, solvent selection,[9,34] catalyst regeneration and reuse[1,3,7,10,11,18,21] will be discussed in Section four. Modelling of sugar transformation kinetics will be also covered.[9] A major part of the sugar transformations has been investigated in batch reactors,[3,7,9] although some publications report continuous operation.[23] Finally some remarks regarding the future research needs will be given.

2. Catalytic Methods to Produce Lactic Acid and Alkyl Lactates from Different Feedstock

2.1. Production of alkyl lactates and lactic acid from sugars and carbohydrates

Sugar transformations to alkyl lactates have been intensively investigated in the recent years[3,7–11,30,33] (Table 1) and mostly Sn-modified zeolites and hierarchical zeolites have been applied as catalysts.[3,7,8] Typically sugar transformations were performed at 160 °C in alcohols[13] using relatively diluted concentrations and reaction time varying from 2–20 h. In water complete glucose conversion was obtained even after 0.5 h at 200 °C.[33] The carbon balance of the glucose transformation reaction mixture in water, determined by total organic carbon (TOC) method, was incomplete, for example, 80% over Zn—Sn-Beta at 190 °C[34] and only 70% at 200 °C over Sn-Beta.[33] In addition, all products are not visible when applying HPLC and GC methods. This results in the sum of the products analysed by HPLC and GC of ca. 70% at 100% conversion of glucose over K—Sn-USY in methanol at 170 °C (Table 1, entry 17)[30] and only 47% over Mg-MOF-74 at 220 °C in methanol.[10] These results show clearly that the carbon balance is not complete.

In several papers only the yields of ML and conversion is given, without reporting formation of other products.[4,7,14] The yields of ML from glucose, vary from 13 to 58% (Table 1, entries 1–28).[3,8] In Ref. [7] high conversions close to 100% have been reported giving ca. 52% ML yield, while information about other products was missing (Table 1, entry 1). Lower lactate yields were reported as expected with ethanol and n-butanol (Table 1, entries 3, 4, 7–11)[4,21,32] due to slower reaction rates with a longer chain alcohol.

The presence of products other than ML or LA is often not given,[1,4,13] making a fair comparison difficult. A relatively high yield of ML, 47%, was obtained over Sn-Beta(150) as a catalyst in glucose transformation at 160 °C in 12 h (Table 1, entry 15).[9] Over alkali modified K—Sn-USY the yield of ML was 40% and

ChemSusChem

Reviews
doi.org/10.1002/cssc.202001223

Chemistry
Europe
European Chemical
Societies Publishing

relatively high amounts of other products, catalysed by Brønsted acid sites, were formed (Table 1, entry 17).[30] It was reported in Refs. [9] and [30] that strong Brønsted acid sites catalyse glucose etherification in alcohols forming alkyl glucosides (Figure 1b). The ML yield at 220 over Mg-MOF-74 was 35% and minor amounts of fructose methyl glycolate and glycolaldehyde dimethylacetal were formed (Table 1, entry 26).[10] Other reported products in glucose transformations in water besides LA were levulinic acid, xylitol and 5-hydroxymethylfurfural (HMF) (Table 1, entry 19).[33] Levulinic acid and HMF can be formed over Brønsted acidic catalysts, while xylitol is formed from fructose isomerization product via C1-C2 cleavage.[44] The highest amounts of acetals were formed over γ-NiOOH (Ni/2-Hmim-4),[11] Fe_2O_3/SnO_2,[35] Mg-MOF-26,[10] K—Sn-USY.[30] It was pointed out in Ref. [18] that pyruvaldehyde acetal can react reversibly at longer reaction times forming ML.

Fructose transformations give typically a higher yield of ML in comparison to glucose transformations[3–7,18,35] since no isomerization step is required. Noteworthy is also that xylose as a feedstock gave lower ML yield in comparison to glucose over Sn-Beta-H (Table 1, entries 1 and 43),[7] while comparative yields of ML were obtained over Sn-Beta-H-0.3 for fructose, xylose and even for sucrose (Table 1, entries 34, 42, 50).[3] In water the yield of LA was about the same from glucose and fructose over Sn-Beta catalyst at 200 °C (Table 1, entries 18 and 33)[33] and the yield of ML from sucrose was slightly lower than from glucose (Table 1, entries 54 and 18).[8]

Typically, monosaccharides react faster than disaccharides, such as sucrose, lactose and maltose to ML,[8,11] although some exceptions have been reported.[3,21] Sucrose afforded high ML yields varying in the range of 11–72% (Table 1, entries 46–57). ML yield from sucrose was higher than that from glucose over other hierarchical Sn-Beta catalysts (Table 1, entries 9 and 51)[21] and in[3] (Table 1, entries 2 and 50)[3,21] as well as over $Fe_2O_3/$

SnO_2 (Table 1, entries 25 and 46).[35] A slightly lower ML yield was obtained from sucrose over hierarchical Sn-Beta-9 h in comparison to glucose (Table 1, entries 6 and 49)[4] as well as over dealuminated Sn-Beta (Table 1, entries 14 and 56),[8] over γ-NiOOH (Ni-2Hmim) (Table 1, entries 40 and 54),[11] and Sn-MWW-nano (Table 1, entries 12 and 52)[13] in comparison to glucose (Table 1, entries 11 and 26). Slower sucrose transformations compared to that of glucose transformation were stated to be originated from a slow disaccharide methanolysis rate under these conditions.[11] A comparative study of maltose and sucrose transformation to ML over Mg-MOF-74 gave similar results (Table 1, entries 53 and 62), while lactose transformations proceeded slowly to ML (Table 1, entries 66 and 67). Noteworthy is that the inulin transformation was efficient over Sn/salen/IL catalyst even after 2 h (Table 1, entry 68), while for Sn-Beta-H it was slow after 20 h (Table 1, entry 69).[21] On the other hand, one explanation of a faster rate for sucrose transformations in comparison to glucose and fructose was slow hydrolysis of sucrose thus lowering monomer concentration and suppressing side reactions over Sn-Beta (Table 1, entries 1, 32, 47).[7]

Trioses are typically transformed very fast to ML (Table 1, entries 71–77). 1,3-Dihydroxyacetone transformations to ML give high yields (Table 1, entries 71–77), because the reaction route to ML involves much fewer steps in comparison to glucose or fructose transformations.[3,13,14,33] For example, it was possible to transform 1,3-dihydroxyacetone to ML with the yield of 47% after 7 h at 80 °C (Table 1, entry 78).[16]

As a conclusion, it can be stated that monomeric sugars, glucose, fructose and xylose gave maximally 58–67% yields of ML typically at 160 °C during 6–20 h over hierarchical Sn-Beta catalysts, while in water the reaction times were much shorter, being 0.5 h. Other metal modified catalysts were also promising. Disaccharides typically reacted slightly slower than monomers,

Päivi Mäki-Arvela received her Doctor of Technology (chemical engineering) in 1994 at Åbo Akademi University, Turku, Finland. Her research areas are catalytic three-phase reactions, especially transformations of renewable raw materials to valuable products using heterogeneous catalysts. She has published more than 330 peer-reviewed publications, several review papers, and patents. Her research has been acknowledged by several prizes. She has served as President of the Nordic Catalysis Society and the Finnish Catalysis Society and a board member in the European Federation Catalysis Societies.

Atte Aho received his Doctor of Technology (chemical engineering) in 2009 at Åbo Akademi University, Finland. His research topics are catalytic transformations of renewable feedstock and physico-chemical characterization of heterogeneous catalysts. He has published nearly 100 peer-reviewed journal articles.

Dmitry Yu. Murzin studied Chemical Technology at the Mendeleev University of Chemical Technology in Moscow, Russia (1980–1986), and graduated with honours. He obtained his PhD (advisor Prof. M.I. Temkin) and DrSc degrees at Karpov Institute of Physical Chemistry, Moscow, in 1989 and 1999, respectively. He worked at Universite Louis Pasteur, Strasbourg, France, and Åbo Akademi University, Turku, Finland, as a post-doc. In 1995–2000 he was associated with BASF, being involved in research, technical marketing and management. Since 2000 he holds the Chair of Chemical Technology at Åbo Akademi University. He is an elected member of Academia Europaea, the Finnish Academy of Science and Letters and holds honorary professorships from Tianjin University, China, and St. Petersburg State Technological Institute, Russia. Prof. Murzin is an author or co-author of ca. 800 journal articles and book chapters as well as several textbooks.
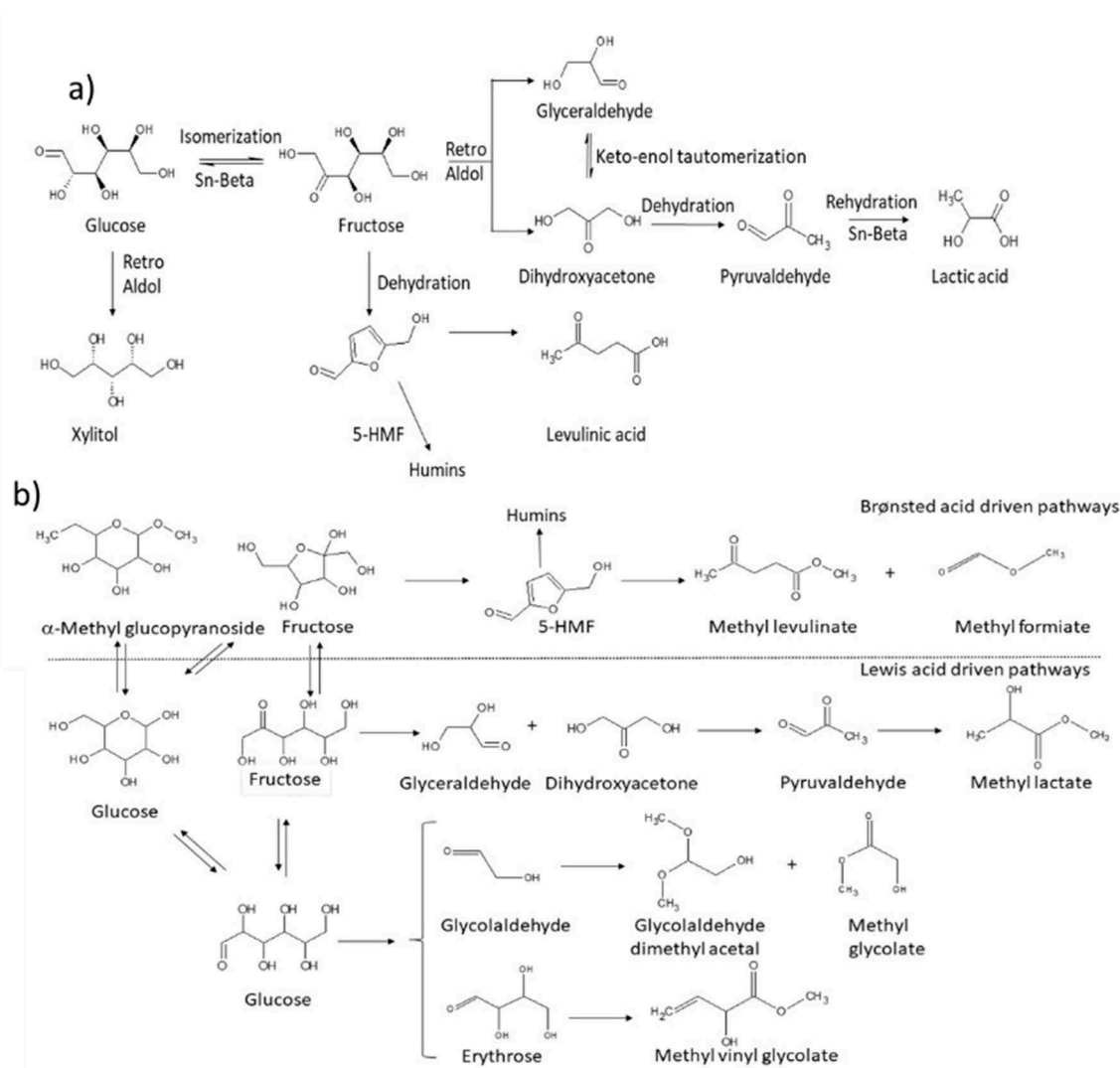
ChemSusChem

Reviews
doi.org/10.1002/cssc.202001223

Chemistry
Europe
European Chemical
Societies Publishing

Figure 1. The main reaction pathways for synthesis of a) lactic acid adapted from Ref. [33] and methyl lactate from glucose, adapted from Ref. [30].

although some exceptions were reported. The challenge is a low carbon balance, being ca. 80% in water while in methanol it can be even lower. ML yield from trioses is higher than from the sugar, maximally close to 100% due to a less demanding reaction network, not requiring retro-aldol condensation of sugars.

3. Catalyst Selection

3.1. Catalyst selection for glucose transformation to alkyl lactate and lactic acid

Different Sn-modified microporous zeolites, such as mordenite, Beta, MWW and MFI were used for transformations of sugars to ML.[4,13] Due to a relatively large size of glucose with the kinetic diameter of 0.86 nm[45] in comparison to the zeolite pore sizes, also metal modified hierarchical zeolites have been demonstrated as efficient catalysts for transformation of sugars to alkyl

lactates[1,3,4,7–9,21,23,30] and LA.[33,34] In addition, several other catalysts, for example, Fe-doped SiO$_2$,[35] Mg-MOF-74,[10] NiO,[12] γ-NiOOH,[11] γ-Al$_2$O$_3$,[14] In-γ-Al$_2$O$_3$,[6] Zr-SBA-15[5] were successfully applied as catalysts for the same reaction (Tables 2 and 3). Several catalysts are quite stable in sugar transformations, for example, NiO[10] and γ-NiOOH,[11] and Sn-Beta even in water[33] although minor leaching occurred from In–γ-Al$_2$O$_3$.[6] (see Section 4.2) and in continuous sugar transformation over Sn—H-Beta in the presence of a small amount of water (see Section 6).[23]

Metal-modified microporous zeolites, such as Sn-MWW, Sn-MOR and Sn-MFI[13] and Sn-Beta prepared via the hydrothermal route in the presence of fluoride[3,4] have been tested in glucose transformation. The results with Sn-modified medium pore size zeolites, MOR, MFI and MWW with the largest cavity size of 0.645 nm, 0.7 nm and 0.492 nm, respectively,[13] gave 20%, 21% and 19% yield of ML, respectively (Table 2, entry 28–30). Only for Sn-MWW catalyst a lower yield of ML was obtained than for its hierarchical counterparts (see below), while for MOR and MFI

ChemSusChem

Reviews
doi.org/10.1002/cssc.202001223

**Chemistry
Europe**
European Chemical
Societies Publishing

Table 1. Highest yield of methyl lactate in transformation of sugars and their derivatives in different studies.[a]

Entry	Catalyst	Conditions	X [%]/Y of other products [%]	$Y_{ML/LA}$[b] [%]	Ref.
Glucose					
1	Sn-Beta, H	5 bar N_2, 160 °C, 0.137 mol L^{-1}, glu/cat 1.6 wt/wt	n.a.	52	[7]
2	Sn-Beta-H-0.3	5 bar N_2, 160 °C, 0.14 mol L^{-1}, glu/cat 1.6 wt/wt, 10 h	99	58	[3]
3	Sn-Beta-H-0.3	5 bar N_2, 160 °C, 0.14 mol L^{-1}, glu/cat 1.6 wt/wt, 10 h, ethanol	100	41[c]	[3]
4	Sn-Beta-H-0.3	5 bar N_2, 160 °C, 0.14 mol L^{-1}, glu/cat 1.6 wt/wt, 10 h, *n*-butanol	100	29[d]	[3]
5	Sn-Beta-4 h	5 bar N_2, 160 °C, 0.08 mol L^{-1}, glu/cat 1.6 wt%/wt%, 10 h		48	[4]
6	Sn-Beta-9 h	5 bar N_2, 160 °C, 0.08 mol L^{-1}, glu/cat 1.6 wt/wt, 10 h,		43	[4]
7	Sn-Beta-9 h	5 bar N_2, 160 °C, 0.08 mol L^{-1}, glu/cat 1.6 wt/wt, 10 h, ethanol		29[c]	[4]
8	Sn-Beta-9 h	5 bar N_2, 160 °C, 0.08 mol L^{-1}, glu/cat 1.6 wt%/wt%, 10 h, *n*-butanol		20[d]	[4]
9	Sn-Beta-H	10 bar N_2, 160 °C, 0.125 mol L^{-1}, glu/cat 1.4 wt/wt, 20 h	$X=97$, $Y_{MVG}=1$	52	[21]
10	Sn-Beta-H	10 bar N_2, 160 °C, 0.125 mol L^{-1}, glu/cat 1.4 wt/wt, 20 h, ethanol		38[c]	[21]
11	Sn-Beta-H	10 bar N_2, 160 °C, 0.125 mol L^{-1}, glu/cat 1.4 wt/wt, 20 h, *n*-butanol		25[d]	[21]
12	Sn-MWW-nano	10 bar N_2, 160 °C, 0.12 mol L^{-1}, glu/cat 1.4 wt/wt, 20 h		36	[13]
13	deAl–Sn-Beta (100)	160 °C,[e] 5 h, 0.14 mol L^{-1}, 3 wt% glucose in MeOH, 1 wt% catalyst		13	[8]
14	deAl–Sn-USY (25)	160 °C,[e] 0.14 mol L^{-1}, 3 wt% glucose in MeOH, 1 wt% catalyst, 5 h		13	[8]
15	Sn-Beta-(150) HT, (HF)	160 °C,[e] 0.132 mol L^{-1}, glu/cat 2.4 wt/wt, 12 h	$X=100$, $Y_{Me-Fru}=4$	47	[9]
16	Sn-Beta	5 bar N_2, 160 °C, 0.137 mol L^{-1}, 10 h		47	[4]
17	K–Sn-USY	170 °C,[e] 0.26 mol L^{-1}, glu/cat 2.4 wt/wt, 6 h, MW	$X=98$, $Y_{GADMA}=9$, $Y_{MG}=3$, $Y_{MeLE}=11$, $Y_{MVG}=9$, carbon balance 63 mol%	40	[30]
18	Sn-USY	160 °C,[e] 0.13 mol L^{-1}, glu/cat 2.4 wt/wt, 2 h, MW		32	[8]
19	Sn-Beta (mesoporous)	40 bar He, 200 °C, 0.11 mol L^{-1}, glu/cat 0.750 wt/wt, 0.5 h, water	$X=98$, $Y_{xyl}=3.5$, $Y_{LeA}=3.1$, $Y_{HMF}=5.1$	58	[33]
20	1Mg–Sn-Beta	4 bar N_2, 160 °C, 0.14 mol L^{-1}, glu/cat 1.9 wt/wt, 5 h	99	48	[1]
21	Zn–Sn-Beta	10 bar, 190 °C, 0.12 mol L^{-1}, glu/cat 1.4 wt/wt, 2 h, water	$X=99$, $Y_{LeA}=3$, $Y_{HMF}=6$, furfural deriv. 3, traces of acetic, formic acids, acetol	45	[34]

ChemSusChem

Reviews
doi.org/10.1002/cssc.202001223

**Chemistry
Europe**
European Chemical
Societies Publishing

Table 1.	continued				
Entry	Catalyst	Conditions	X [%]/Y of other products [%]	$Y_{ML/LA}$[b] [%]	Ref.
22	Zr-SBA-15	27.6 bar N_2, 240 °C, 0.06 mol L^{-1}, glu/cat 2.0 wt/wt, 6 h		37	[5]
23	Al$_2$O$_3$, calcined at 500 °C	5 bar Ar, 160 °C, 0.06 mol L^{-1}, 6 h	< 99	34	[14]
24	Sn/(salen)IL	20 bar N_2, 160 °C, 0.11 mol L^{-1}, glu/cat 6 wt/wt, 4 h	$Y_{MeLe}=2$, $Y_{PADA}=1$, $Y_{MMF}=2$	40	[18]
25	Fe$_2$O$_3$-SnO$_2$ with 0.2 molar ratio of Fe/(Fe + Sn)	10 bar, 160 °C, 0.06 mol L^{-1}, glu/cat 1.4 wt/wt, 20 h	$X=99$, $Y_{PADA}=7$	35	[35]
26	Mg-MOF-74	220 °C,[e] 0.037 mol L^{-1}, glu/cat 3.0 wt/wt, 3 h, near critical methanol	$X=100$, $Y_{MG+GADMA}=9$, $Y_{fru}=2$	35	[10]
27	12 wt% In/Al$_2$O$_3$	180 °C, 0.03 mol L^{-1}, glu/cat 2.0 wt/wt, 10 h, methanol/water 13.2 v/v, K$_2$CO$_3$	$Y_{HMF}=4$, $Y_{MG}=3$, $Y_{PADA}=5$	42	[6]
28	γ—NiOOH (Ni/2-Hmim-4)	200 °C,[e] 0.044 mol L^{-1}, glu/cat 2 wt/wt, 3 h	$X=100$, $Y_{GAGMA+MG}=13$, $Y_{APG}=2$, $Y_{fru}=7.5$	40	[11]
Fructose					
29	Sn-Beta-H	10 bar N_2, 160 °C, 0.125 mol L^{-1}, fru/cat 1.4 wt/wt, 20 h	$Y_{MVG}=1$	51	[21]
30	Sn-Beta-9 h	5 bar N_2, 160 °C, 6 h, 0.08 mol L^{-1}, fru/cat 1.6 wt/wt, 10 h		47	[4]
31	Sn-MWW-nano	10 bar N_2, 160 °C, 0.12 mol L^{-1}, fru/cat 1.4 wt/wt, 20 h		40	[13]
32	Sn-Beta, H	5 bar N_2, 160 °C, 6 h, 0.137 mol L^{-1}, fru/cat 1.6 wt/wt	n.a.	58	[7]
33	Sn-Beta (mesoporous)	40 bar He, 200 °C, 0.11 mol L^{-1}, fru/cat 0.75 wt/wt, 0.5 h, water	$X=98$, $Y_{xyl}=3.1$, $Y_{LeA}=3.2$, $Y_{HMF}=3.4$	58	[33]
34	Sn-Beta-H-0.3	5 bar N_2, 160 °C, 10 h, 0.137 mol L^{-1}, fru/cat 1.6 wt/wt	$X=95$, pyruvald addition products 30	41	[3]
35	1Mg—Sn-Beta (mesoporous)	4 bar N_2, 160 °C, 0.14 mol L^{-1}, fru/cat 1.85 wt/wt, 1 h		37	[1]
36	Sn(salen)/IL	20 bar N_2, 160 °C, 4 h, 0.11 mol L^{-1}, fru/cat 6 wt/wt, 2 h	$X=100$, $Y_{MeLe}=2$, $Y_{PADA}<1$, $Y_{MMF}=5$, $Y_{MG}=5$	68	[18]
37	Mg-MOF-74	220 °C, 0.06 mol L^{-1}, fru/cat 3.0 wt/wt, 3 h, near critical methanol	$Y_{MG+GADMA}=8$	37	[10]
38	Zr-SBA-15	27.6 bar N_2, 240 °C, 0.06 mol L^{-1}, fru/cat 2.0 wt/wt, 6 h		44	[5]
39	Fe$_2$O$_3$-SnO$_2$ with 0.2 molar ratio of Fe/(Fe + Sn)	10 bar, 160 °C, 0.06 mol L^{-1}, fru/cat 1.4 wt/wt, 20 h		52	[35]
40	γ—NiOOH (Ni/2-Hmim-4)	200 °C,[e] 0.044 mol L^{-1}, fru/cat 2 wt/wt, 12 h	$X=100$, $Y_{GADMA+MG}=11$, $Y_{APG}=2$	47	[11]
41	NiOOH	200 °C,[e] 0.03 mol L^{-1}, fru/cat 6 wt/wt, 3 h		42	[12]
Xylose					
42	Sn-Beta-H-0.3	5 bar N_2, 160 °C, 0.014 mol L^{-1}, xyl/cat 1.6 wt/wt, 10 h	$X=100$	53	[3]

ChemSusChem

Reviews
doi.org/10.1002/cssc.202001223

**Chemistry
Europe**
European Chemical
Societies Publishing

Table 1. continued

Entry	Catalyst	Conditions	X [%]/Y of other products [%]	$Y_{ML/LA}$[b] [%]	Ref.
43	Sn-Beta, H	5 bar N$_2$, 160 °C, 0.164 mol L^{-1}, xyl/cat 1.6 wt/wt, 6 h	n.a.	40	[7]
44	Sn-Beta (mesoporous)	40 bar He, 200 °C, 0.13 mol L^{-1}, xyl/cat 0.75, water wt/wt, 0.5 h	$X=99$, 1,2-propanediol, 1,3-propanediol	67	[33]
45	Zr-SBA-15	27.6 bar N$_2$, 240 °C, 0.07 mol L^{-1}, xyl/cat 2.0 wt/wt, 10 h	$Y_{GADMA}=2$	37	[5]
46	Fe$_2$O$_3$-SnO$_2$ with 0.2 molar ratio Fe$_2$O$_3$ to SnO$_2$	10 bar, 160 °C, 0.06 mol L^{-1}, suc/cat 1.4 wt/wt, 20 h	$Y_{PADA}=4$	60	[35]
Sucrose					
47	Sn-Beta, H	5 bar N$_2$, 160 °C, 0.007 mol L^{-1}, suc/cat 1.6 wt/wt, 6 h	n.a.	67	[7]
48	Sn/(salen)IL	20 bar N$_2$, 160 °C, 0.063 mol L^{-1}, suc/cat 6 wt/wt, 4 h	$Y_{MeLe}=2$, $Y_{MMF}=3$, $Y_{MG}=3$	52	[18]
49	Sn-Beta-9 h	5 bar N$_2$, 160 °C, 0.08 mol L^{-1}, suc/cat 1.6 wt/wt, 10 h		57	[4]
50	Sn-Beta-H-0.3	5 bar N$_2$, 160 °C, 0.07 mol L^{-1}, suc/cat 1.6 wt/wt, 10 h	$X=100$	50	[3]
51	Sn-Beta-H	10 bar N$_2$, 160 °C, 0.125 mol L^{-1}, suc/cat 1.4 wt/wt, 20 h	$Y_{MVG}=2$	71	[21]
52	Sn-MWW-nano	10 bar N$_2$, 160 °C, 0.06 mol L^{-1}, suc/cat 1.4 wt/wt, 20 h		28	[13]
53	Mg-MOF-74	220 °C, 0.02 mol L^{-1}, suc/cat 3.0 wt/wt, 3 h, near-critical methanol	$Y_{MG+GADMA}=5$, $Y_{fru}=2$	46	[10]
54	γ—NiOOH (Ni/2-Hmim-4)	200 °C,[e] 0.023 mol L^{-1}, suc/cat 2 wt/wt, 12 h	$X=100$, $Y_{GADMA+MG}=8$, $Y_{APG}=6$	38	[11]
55	Sn-Beta (mesoporous)	40 bar He, 200 °C, 0.06 mol L^{-1}, suc/cat 0.75 wt/wt, 0.5 h	$X=98$, $Y_{xyl}=3.2$, $Y_{LeA}=3.8$, $Y_{HMF}=3.7$	55	[33]
56	deAl—Sn-USY (25)	160 °C,[e] 0.14 mol L^{-1}, 3 wt% sucrose in MeOH, 1 wt% catalyst, 5 h		11	[8]
57	Sn-Beta-H	10 bar N$_2$, 160 °C, 0.06 mol L^{-1}, suc/cat 1.4 wt/wt, 20 h	traces of MVG	72	[21]
58	Fe$_2$O$_3$-SnO$_2$ with 0.2 molar ratio of Fe/(Fe+Sn)	10 bar, 160 °C, 0.03 mol L^{-1}, suc/cat 1.4 wt/wt, 20 h	$Y_{PADA}=12$	33	[35]
59	Zr-SBA-15	28 bar N$_2$, 240 °C, 0.04 mol L^{-1}, suc/cat 2.0 wt/wt, 6 h			[5]
Maltose					
60	Sn-Beta, H	5 bar N$_2$, 160 °C, 0.007 mol L^{-1}, malt/cat 1.6 wt/wt, 6 h	n.a.	36	[7]
61	Sn-Beta-H	10 bar N$_2$, 160 °C, 0.125 mol L^{-1}, malt/cat 1.4 wt%/wt%, 20 h	traces of MVG	32	[21]
62	Mg-MOF-74	220 °C,[e] 0.02 mol L^{-1}, mal/cat 3.0 wt/wt, 3 h, near-critical methanol	$Y_{MG+GADMA}=5$	17	[10]
63	γ—NiOOH (Ni/2-Hmim-4)	200 °C,[e] 0.023 mol L^{-1}, mal/cat 2 wt/wt, 12 h	$X=88$, $Y_{GAGMA+MG}=9$, $Y_{APG}=16$	22	[11]

Table 1. continued

Entry	Catalyst	Conditions	X [%]/Y of other products [%]	$Y_{ML/LA}$[b] [%]	Ref.
64	Mg-MOF-74	220 °C, 0.02 mol L^{-1}, mal/cat 3.0 wt/wt, 6 h, near-critical methanol		47	[10]
Maltotriose					
65	Sn-Beta-H	10 bar N$_2$, 160 °C, 0.04 mol L^{-1}, maltotr./cat 1.4 wt/wt, 20 h		10	[21]
Lactose					
66	Mg-MOF-74	220 °C, 0.02 mol L^{-1},[e] lac/cat 3.0 wt/wt, 3 h, near-critical methanol	$Y_{MG+GADMA} = 9$	17	[10]
67	γ−NiOOH (Ni/2-Hmim-4)	200 °C, 0.023 mol L^{-1}, lac/cat 2 wt/wt, 12 h	$X = 100$, $Y_{GAGMA+MG} = 8$, $Y_{APG} = 6$	17	[11]
Inulin					
68	Sn/(salen)/IL	20 bar N$_2$, 160 °C, 2.4 wt%, inu/cat 6 wt/wt, 2 h		60	[18]
69	Sn-Beta-H	10 bar N$_2$, 160 °C, 2 wt%, inu/cat 1.4 wt/wt, 20 h		22	[21]
70	deAl−Sn-USY(25)	160 °C, 3 wt%, 1 wt% cat, 4 h	$Y_{Me-fruc} = 16$, $Y_{MVG} = 2$	23	[8]
1,3-dihydroxyacetone					
71	[Sn]-Beta-HF	5 bar N$_2$, 160 °C, 0.25 mol L^{-1}, dha/cat 14 wt/wt, 2 h		99	[13]
72	Sn-Beta-H-0.3	5 bar N$_2$, 160 °C, 0.014 mol L^{-1}, DHA/cat 1.6 wt/wt, 10 h	< 99	89	[3]
73	Sn-Beta	4 bar N$_2$, 160 °C, 0.27 mol L^{-1}, dha/cat 1.85 wt/wt, 10 h	98	77	[1]
74	Sn(salen)/IL	20 bar N$_2$, 160 °C, 0.22 mol L^{-1}, DHA/cat 6 wt/wt, 2 h	100	93	[18]
75	NiO	200 °C, 0.11 mol L^{-1}, DHA/cat 2 wt/wt, 3 h	n.a.	72	[12]
76	Zr-SBA-15	27.6 bar N$_2$, 240 °C, 0.11 mol L^{-1}, DHA/cat 2.0 wt/wt, 1 h		84	[5]
77	Al$_2$O$_3$, calcined at 500 °C	5 bar Ar, 160 °C, 0.06 mol L^{-1}, h	< 99	62	[14]
78	Sn/Al$_2$O$_3$	molar ratio DHA/ethanol = 0.023, w_{cat}/w_{DHA} = 43 wt %, 80 °C, 7 h, ethanol	$X = 99\%$, $Y_{GLADA} = 17$, $Y_{PADA} = 11$, $Y_{PA} = 9$	48	[16]

[a] X = conversion, Y = yield, MW = microwaves, MeLa = methyl lactate, LA = lactic acid, LeA = levulinic acid, MeLe = methyl levulinate, HMF = 5-hydroxymethylfurfural, xyl = xylitol, GADMA = glycolaldehyde dimethylacetal, PADA = pyruvaldehyde di(m)ethylacetal, MMF = 5-methoxymethylfurfural, MG = methyl glycolate, MVG = methyl vinyl glycolate, fru = fructose, PDO = propanediol, APG = methyl-α-D-glucopyranoside/methyl-β-D-glucopyranoside, GLADA = glyceraldehyde diethyl acetal, TPAOH = tetrapropylammoniumhydroxide. [b] Methyl lactate when solvent methanol, lactic acid when solvent water. [c] Ethyl lactate. [d] Butyl lactate. [e] Pressure not given.

no such clear trends were visible (Figure 2).[13] One possible explanation for the high activity of MWW and MFI zeolites based on DFT calculation is that stabilization of carbohydrate intermediates requires 174–200 kJ mol^{-1} for large pore zeolites, Sn-Beta and Sn-MOR, while for small pore zeolites Sn-MFI and Sn-MWW the corresponding energy is 220–240 kJ mol^{-1} when

taking into account correction for van der Waals interactions.[47] It was concluded in Ref. [13] that retro-aldolization could not be improved using hierarchical zeolites.

For Sn-modified large pore zeolite Sn-Beta a higher yield of ML, 47%, was obtained in comparison with Al-Beta, 3% (Table 2, entries 1 and 3), which is related to lower amounts of

ChemSusChem

Reviews
doi.org/10.1002/cssc.202001223

Chemistry Europe
European Chemical
Societies Publishing

Table 2. Yield of methyl lactate over different catalysts together with the concentration of Lewis acid sites and the ratio between mesopore (V_{meso}) vs micropore volume (V_{micro}) of the catalyst.[a]

Entry	Catalyst	Catalyst preparation method	Conditions in glucose transformation	Catalyst properties	V_{meso}/V_{micro}	Lewis acid sites [mmol g_{cat}^{-1}]	Yield of MeLa [%]	Ref.
1	Al-Beta	commercial, dealuminated	5 bar N_2, 160 °C, 0.14 mol L^{-1}, glu/cat 1.6 wt/wt, 10 h	Si/Al ratio 19.5	0.40	n.a.	2	[3]
2	Sn-Beta-F, fluoride	hydrothermal route	5 bar N_2, 160 °C, 0.14 mol L^{-1}, glu/cat 1.6 wt/wt, 10 h	large crystal size, large amount of silanol defects	0.41	0.103	33	[4]
3	Sn-Beta-F	hydrothermal route, HF media	5 bar N_2, 160 °C, 0.14 mol L^{-1}, glu/cat 1.6 wt/wt, 10 h	low Sn amount loaded, long crystallization time large particles (1000 nm), pore size 4 nm	0.46	n.a.	47	[3]
4	Si-Beta	dealumination of Beta with HNO_3, calcination	5 bar N_2, 160 °C, 0.137 mol L^{-1}, glu/cat 1.6 wt/wt, 6 h		0.75	n.a.	3	[7]
5	deAl-Beta	dealumination of Beta with HNO_3, calcination	5 bar N_2, 160 °C, 0.14 mol L^{-1}, glu/cat 1.6 wt/wt, 10 h	pore size 4 nm Si/Al ratio 1470	0.58	0.016	10	[3]
6	Sn-Beta-P	deAl-Beta (entry 5) was ground with $SnCl_4 \cdot 5H_2O$, calcined	5 bar N_2, 160 °C, 0.14 mol L^{-1}, glu/cat 1.6 wt/wt, 10 h	too high silanol content, 1.9 wt% Sn pore size 4 nm	0.79	n.a.	19	[3]
7	Hf-Beta	Si-Beta was prepared via dealumination of Beta; thereafter Sn-Beta-H was prepared by dissolution of Si-Beta in TEAOH; $HfOCl_2 \cdot 8H_2O$ was dissolved in ethanol and added dropwise to Si-Beta-TEAOH solution, followed by ethanol evaporation at 65 °C, precrystallization at 140 °C for 45 min, and gel formation via addition of NH_4F; crystallization was performed at 140 °C for 12 h	5 bar N_2, 160 °C, 0.137 mol L^{-1}, glu/cat 1.6 wt/wt, 6 h		0.74	n.a.	20	[7]
8	Zr-Beta	Si-Beta was prepared via dealumination of Beta; thereafter Sn-Beta-H was prepared by dissolution of Si-Beta in TEAOH; $ZrOCl_2 \cdot 8H_2O$ was dissolved in ethanol, added dropwise to Si-Beta-TEAOH solution; ethanol was evaporated at 65 °C, the residue was precrystallized at 140 °C for 45 min, the gel was formed via addition of NH_4F, and crystallization was performed at 140 °C for 12 h	5 bar N_2, 160 °C, 0.137 mol L^{-1}, glu/cat 1.6 t/wt, 6 h		0.8	n.a.	23	[7]
9	Sn-Beta	Si-Beta was prepared via dealumination of Beta; thereafter Sn-Beta-H was prepared by dissolution of Si-Beta in TEAOH; $SnCl_4 \cdot 5H_2O$ was dissolved in ethanol and added dropwise to Si-Beta-TEAOH solution; ethanol was evaporated at 65 °C; after pre-crystallisation at 140 °C for 45 min, the gel was formed via addition of NH_4F; crystallization was performed at 140 °C for 12 h	5 bar N_2, 160 °C, 0.137 mol L^{-1}, glu/cat 1.6 wt/wt, 6 h		0.8	n.a.	33	[7]
10	Sn-Beta-AT (desilicated)	mesoporous Si-Beta was prepared using TEOS as a structure-directing agent, HF was added to form a gel,[52] dealuminated Beta was used as a seed, washed and calcined; TEAOH was used to form Si-Beta-AT, which was ground with $SnCl_4 \cdot 5H_2O$ and calcined	5 bar N_2, 160 °C, 0.137 mol L^{-1}, 10 h	large amounts of silanol large amount of Sn in framework	0.44	0.115	32	[4]
11	Sn-Beta-H-0.05[b]	dealuminated Beta zeolite was ground with $SnCl_4 \cdot 5H_2O$ and thereafter crystallized in the presence of TEAOH at 140 °C as a structure-directing agent for 24 h, dried and calcined.	5 bar N_2, 160 °C, 0.08 mol L^{-1}, glu/cat 1.6 wt/wt, 10 h, ethanol	1.2 wt% Sn, pore size 6–18 nm	1.21	0.032	38	[3]
12	Sn-Beta-H-0.1[b]	same as in entry 11	5 bar N_2, 160 °C, 0.08 mol L^{-1}, glu/cat 1.6 wt/wt, 10 h, ethanol	1.5 wt% Sn, pore size 6–18 nm, av. size 7.8 nm	0.62	0.046	47	[3]
13	Sn-Beta-H-0.2[b]	same as in entry 11	5 bar N_2, 160 °C, 0.08 mol L^{-1}, glu/cat 1.6 wt/wt, 10 h, ethanol	1.6 wt% Sn, pore size 6–18 nm, av. size 7.8 nm	0.67	0.057	49	[3]

Table 2. continued

Entry	Catalyst	Catalyst preparation method	Conditions in glucose transformation	Catalyst properties	V_{meso}/V_{micro}	Lewis acid sites [mmol g_{cat}^{-1}]	Yield of MeLa [%]	Ref.
14	Sn-Beta-H-0.3[b]	same as in entry 11	5 bar N$_2$, 160°C, 0.08 mol L^{-1}, glu/cat 1.6 wt/wt, 10 h, ethanol	1.7 wt% Sn, pore size 6–18 nm, av. size 7.8 nm	0.84	0.059	58	[3]
15	Sn-Beta-H-0.4[b]	same as in entry 11	5 bar N$_2$, 160°C, 0.08 mol L^{-1}, glu/cat 1.6 wt/wt, 10 h, ethanol	2.3 wt% Sn, pore size 6–18 nm, av. size 7.8 nm	1.74	0.054	57	[3]
16	Sn-Beta-4 h[c]	mesoporous Si-Beta was prepared using TEOS as a structure-directing agent, HF was added to form a gel,[52] dealuminated Beta was used as a seed, washed and calcined; Si-Beta-xh was ground with SnCl$_4$·5H$_2$O and calcined	5 bar N$_2$, 160°C, 0.137 mol L^{-1}, 10 h	no Brønsted acid sites	4.6	0.061	47	[4]
17	Sn-Beta-6 h[c]	same as in entry 16	5 bar N$_2$, 160°C, 0.137 mol L^{-1}, 10 h		2.9	0.060	45	[4]
18	Sn-Beta-9 h[c]	same as in entry 16	5 bar N$_2$, 160°C, 0.137 mol L^{-1}, 10 h	high Sn amount loaded with long crystallization time, 300 nm particles, pore size 5–60 nm	0.74	0.067	43	[4]
19	5Sn-Beta-9 h[c]	Same as in entry 16, but with different amount of Sn precursor	5 bar N$_2$, 160°C, 0.137 mol L^{-1}, 10 h		0.87	0.098	42	[4]
20	Sn-Beta-H1[c]	Si-Beta was prepared via dealumination of Beta; thereafter Sn-Beta-H was prepared by dissolution of Si-Beta in TEAOH; SnCl$_2$·H$_2$O was dissolved in ethanol and added dropwise to Si-Beta-TEAOH solution; PDADMAC was added as a mesoporous structure-directing agent for Si-Beta; ethanol was evaporated at 65°C; after precrystallization at 140°C for 45 min, the gel was formed via addition of NH$_4$F; crystallization was performed at 140°C for 12 h	5 bar N$_2$, 160°C, 0.137 mol L^{-1}, glu/cat 1.6 wt/wt, 6 h	pore size between 5–55 nm	1.1	n.a.	36	[7]
21	Sn-Beta-H2[d]	same as in entry 20	5 bar N$_2$, 160°C, 0.137 mol L^{-1}, glu/cat 1.6 wt/wt, 6 h	pore size between 5–55 nm	1.8	n.a.	42	[7]
22	Sn-Beta-H4[d]	same as in entry 20	5 bar N$_2$, 160°C, 0.137 mol L^{-1}, glu/cat 1.6 wt/wt, 6 h	pore size between 5–55 nm less silanol groups desorbed between 673–1073 K, more Sn in framework, increased d spacing in TEM image	2.8	0.054	52	[7]
23	Zr-Beta-H4[d]	same as in entry 20, precursor ZrOCl$_2$·8H$_2$O	5 bar N$_2$, 160°C, 0.137 mol L^{-1}, glu/cat 1.6 wt/wt, 6 h		2.8	0.035	37	[7]
24	Hf-Beta-H4[d]	same as in entry 20, precursor HfOCl$_2$·8H$_2$O	5 bar N$_2$, 160°C, 0.137 mol L^{-1}, glu/cat 1.6 wt/wt, 6 h		2.9	0.028	34	[7]
25	Meso-Sn-Beta	dealumination of Beta zeolite was performed with oxalic acid followed by desilication with alkali; the next step was treatment with concentrated HNO$_3$ to obtain siliceous meso-Si-Beta on which organometallic Sn was incorporated via grinding and calcination	5 bar N$_2$, 160°C, 0.137 mol L^{-1}, glu/cat 1.6 wt/wt, 6 h	I_{eff}[e] = 61%, Sn content 158 μmol g^{-1}, large amount of silanol groups	2.9	0.165	15	[13]
26	Sn-MFI-bulk-F	to SnCl$_4$·5H$_2$O solution NH$_4$F was added and stirred; the prepared solution was added into TPABr and TPAOH solution and stirred; thereafter fumed silica was added into this solution and crystallization was performed at 200°C for 11 days and calcined[29]	10 bar N$_2$, 160°C, 0.12 mol L^{-1}, glu/cat 1.4 wt/wt, 20 h	n.a.	0.14	n.d.	29	[13]
27	Sn-Beta-HF	synthesis in HF media[53]: TEOS and TEAOH stirred with aqueous SnCl$_4$·5H$_2$O followed by addition of HF; dealuminated Beta was used as a seed; crystallization was	a) 10 bar N$_2$, 160°C 0.12 mol L^{-1}, glu/	2000 nm particles	0.27	n.d.	30	[13]

Table 2. continued								
Entry	Catalyst	Catalyst preparation method	Conditions in glucose transformation	Catalyst properties	V_{meso}/V_{micro}	Lewis acid sites [mmol g_{cat}^{-1}]	Yield of MeLa [%]	Ref.
		performed at 140 °C for a) 40 days in static, b) 20 h in rotating form; the material was dried and calcined	cat 1.4 wt/wt, 20 h					
			b) 160 °C, 0.132 mol L^{-1}, glu/cat 2.4 wt/wt, 12 h	specific surface area 602 m^2 g$_{cat}^{-1}$ all Sn in framework	n.d.	n.d.	47	[9]
28	Sn-MOR-bulk	anhydrous SnCl$_4$ was incorporated via mixing it with dealuminated and dried zeolite and allowing the mixture to stand at 100 °C for 16 h under an inert atmosphere; thereafter the mixture washed collected and washed with methanol, dried and calcined	10 bar N$_2$, 160 °C, 0.12 mol L^{-1}, glu/cat 1.4 wt/wt, 20 h	$I_{eff}^{[e]}$ = 33 %, low amount of framework Sn, low amount of mesopores, Sn content 471 μmol g^{-1}, 2000 nm particles Si/Al ratio 138	1.1	0.281	20	[13]
29	Sn-MFI-bulk	Sn incorporated to MFI-bulk similar as in entry 28	10 bar N$_2$, 160 °C, 0.12 mol L^{-1}, glu/cat 1.4 wt/wt, 20 h	$I_{eff}^{[e]}$ = 60 %, low amount of framework Sn, Sn content 57 μmol g^{-1} Si/Al ratio 53	0.62	0.085	21	[13]
30	Sn-MWW-bulk	silica gel was mixed with hexamethyleneimine into which NaOH and NaAlO$_2$ were added and the mixture was stirred; crystallization was performed at 150 °C for 7 days and thereafter the material was calcined; Sn incorporated similar as in entry 26	10 bar N$_2$, 160 °C, 0.12 mol L^{-1}, glu/cat 1.4 wt/wt, 20 h	Si/Al ratio 35	1.1	n.d.	19	[13]
31	Sn-MWW-delam	MWW precursor combined with CTAB and mixed with TPAOH; the mixture was ultrasonificated, pH was adjusted to 2; thereafter the material was washed, dried and calcined; Sn incorporated similar as in entry 26	10 bar N$_2$, 160 °C, 0.12 mol L^{-1}, glu/cat 1.4 wt/wt, 20 h	$I_{eff}^{[e]}$ = 61 %, Sn content 464 μmol g^{-1} Si/Al ratio 56	2.1	0.472	30	[13]
32	Sn-MWW-nano	MWW nanoparticles were prepared via mixing silica gel with hexamethyleneimine, thereafter NaOH and sodium aluminate were added and stirred overnight at 25 °C, followed by addition of dimethyloctadecyl[(trimethylsilyl)propyl]ammonium chloride, stirred for 4 h, crystallization at 150 °C for 7 days, rotation, calcination; Sn incorporated similar as in entry 26	10 bar N$_2$, 160 °C, 0.12 mol L^{-1}, glu/cat 1.4 wt/wt, 20 h	$I_{eff}^{[e]}$ = 54 %, highest Sn content (197 μmol g^{-1}), 200 nm agglomerates composed of 10 nm particles Si/Al ratio 33	5.0	0.279	36	[13]
33	Sn-MFI-nano	TEOS combined with TPAOH mixed with a NaAlO$_2$ solution, refluxed at 90 °C for 6 h; thereafter N-phenyl-aminopropyl-tetrasiloxane was added, crystallization at 170 °C for 5 days, dried and calcined; Sn incorporated similar as in entry 26	10 bar N$_2$, 160 °C, 0.12 mol L^{-1}, glu/cat 1.4 wt/wt, 20 h	$I_{eff}^{[e]}$ = 56 %, low efficiency for Al extraction from MFI, Sn content 172 μmol g^{-1} Si/Al ratio 55	1.1	0.171	23	[13]
34	Sn-MFI-nanosheet	TEOS-NaOH solution was mixed with C$_{22-6-3}$ template, shaken and stirred; crystallization was performed at 150 °C for 10 days; thereafter the material was dried and calcined; Sn was incorporated similar as in entry 26	10 bar N$_2$, 160 °C, 0.12 mol L^{-1}, glu/cat 1.4 wt/wt, 20 h	2–3 nm thick Si/Al ratio 138	4.0	n.d.	31	[13]
35	Sn-MOR-nano	bulk mordenite was ball milled and ultrasonicated; Sn was incorporated in the same way as in entry 26	10 bar N$_2$, 160 °C, 0.12 mol L^{-1}, glu/cat 1.4 wt/wt, 20 h	300 nm particles Si/Al ratio 160	1.5	n.d.	14	[13]
36	Sn-Beta-nano	dealuminated nanosized Beta was prepared with 65 % HNO$_3$;[20] crystallization occurred at 140 °C for 40 days in static mode; Sn was incorporated in the same way as in entry 26	10 bar N$_2$, 160 °C, 0.12 mol L^{-1}, glu/cat 1.4 wt/wt, 20 h	Si/Al ratio 634	2.4	n.d.	21	[13]
37	Mg-Beta	Mg was loaded on dealuminated Beta via incipient wetness method; then the catalyst was dried and calcined	4 bar N$_2$, 160 °C, 0.14 mol L^{-1}, glu/cat 1.9 wt/wt, 5 h	pore size in range of 5–32 nm	1.7	0.034	12	[1]
38	Sn-Beta	Sn was loaded on dealuminated Beta via incipient wetness method; then the catalyst was dried and calcined	4 bar N$_2$, 160 °C, 0.14 mol L^{-1}, glu/cat 1.9 wt/wt, 5 h	pore size in range of 5–20 nm	2.1	0.055	18	[1]
39	1MgSn-Beta	Mg and Sn were loaded on dealuminated Beta via incipient wetness method; then the catalyst was dried and calcined	4 bar N$_2$, 160 °C, 0.14 mol L^{-1}, glu/cat 1.9 wt/wt, 5 h	large number of silanol groups pore size 3–30 nm	2.0	0.083	46	[1]

Table 2. continued

Entry	Catalyst	Catalyst preparation method	Conditions in glucose transformation	Catalyst properties	V_{meso}/V_{micro}	Lewis acid sites [mmol g_{cat}^{-1}]	Yield of MeLa [%]	Ref.
40	4MgSn-Beta	same as in entry 39	4 bar N_2, 160°C, 0.14 mol L^{-1}, glu/cat 1.9 wt/wt, 5 h	strong basicity pore size in range of 5–32 nm	2.0	0.111	42	[1]
41	Beta	commercial Beta zeolite	10 bar, 190°C, 0.12 mol L^{-1}, glu/cat 1.4 wt/wt, 2 h, water	Si/Al ratio 25	0.88	0.15	5	[34]
42	deAl-Beta	beta was dealuminated with HNO$_3$	10 bar, 190°C, 0.12 mol L^{-1}, glu/cat 1.4 wt/wt, 2 h, water	Si/Al ratio > 1700	2.0	0	3	[34]
43	Zn-Beta	Zn acetate was incorporated on dealuminated Beta zeolite via grinding; the catalyst was thereafter calcined	10 bar, 190°C, 0.12 mol L^{-1}, glu/cat 1.4 wt/wt, 2 h, water	Si/Al ratio > 1700	0.89	0.12	17	[34]
44	Sn-Beta	Sn acetate was incorporated on dealuminated Beta zeolite via grinding; the catalyst was thereafter calcined	10 bar, 190°C, 0.12 mol L^{-1}, glu/cat 1.4 wt/wt, 2 h, water	Si/Al ratio > 1700	0.856	0.13	23	[34]
45	Zn–Sn-Beta	Zn and Sn acetate were incorporated on dealuminated Beta zeolite via grinding; the catalyst was thereafter calcined	10 bar, 190°C, 0.12 mol L^{-1}, glu/cat 1.4 wt/wt, 2 h, water	Si/Al ratio > 1700	0.86	0.17	48	[34]
46	Sn-Beta-C	TEAOH was used as a template, the mixture was stirred for 5 h, crystallization was performed at 140°C for 96 h, followed by drying and calcination	10 bar N_2, 160°C, 0.125 mol L^{-1}, glu/cat 1.4 wt/wt 20 h, ethanol	3.7 wt% Sn, pore size 0.5–1.1 nm	1.2	n.a.	39	[21]

[a] TEOS = tetraethyl orthosilicate, TEAOH = tetraethylammonium hydroxide, PDADMAC = poly(diallyldimethylammonium chloride), CTAB = cetyltrimethylammonium bromide, C_{22-6-3} = diquaternary ammonium salt (DQAS), structure-directing agent of the general type $C_iH_{2i+1}.N^+(CH_3)_2–C_jH_{2j}.N^+(CH_3)_2–C_kH_{2k+1}$ = TPABr. [b] Concentration of TEAOH used for desilication. [c] x h, where x is a number denoting crystallisation time in h; these catalysts were prepared in fluoride media and desilicated with TEAOH to create silanol defects, thereafter Sn was incorporated via solid state ion-exchanged (SSIE), the best catalyst Sn-Beta-4 h. [d] H1, H2, H4 denote different amounts of PDADMAC used as template. [e] I_{eff} (%) = efficiency to incorporate Sn (calculated by amount of Sn per removed Al), it does not take into account potential extra-framework Al.
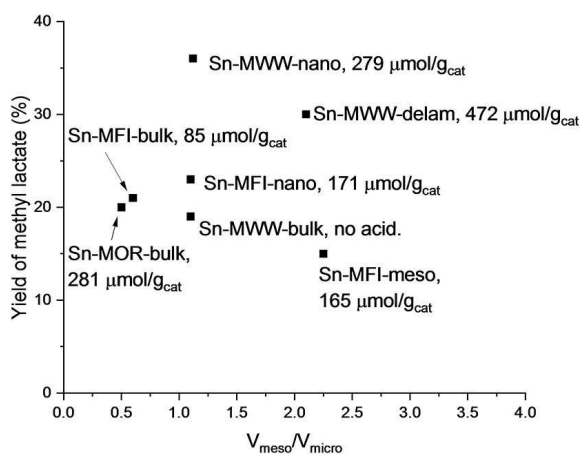

Figure 2. Yields of ML over Sn-MWW-nano, delaminated Sn-MWW, nanosized Sn-MFI, Sn-MFI-meso and Sn-MOR bulk.[13] Conditions: 0.12 mol L^{-1} glucose, glu/cat 1.4 wt/wt at 160°C in 20 h.

Lewis acid sites in Al-Beta (Table 2, entry 1).[3] It was also stated that the zeolite synthesis via the hydrothermal route in fluoride medium creates large particles and can cause diffusional limitations[3] in glucose transformation. When comparing the performance of Sn-Beta-F with the hierarchical Sn-Beta-H-0.3 (Table 2, entries 3 and 14) in[3] the benefit of hierarchical structure was clearly visible opposite to the results (see above) in Ref. [13]. Microporous Sn-Beta prepared in HF medium gave 30% yield of ML in 20 h (Table 2, entry 27a). In this case Sn exclusively in the framework position, which was confirmed by the solid state NMR.[53] On the other hand, Sn-Beta(150)-HF, prepared in an analogous way, but with 20 days crystallization, afforded 47% yield of ML in 12 h (Table 2, entry 27b).[9] This catalyst exhibits a micropore volume of 0.24 ml/g_{cat} which is comparative to the results of[4] obtained over Sn-Beta-4 h, exhibiting mainly mesopores (Table 1, entry 16). Based on this comparison it can be stated that the pore size is not necessary the most determining factor for giving high yields of ML.

Mesoporosity can suppress diffusional limitations of sugars[3,4] during their transformations to LA or alkyl lactates. Several methods exist to create mesoporosity, such as dealumination,[3] desilication[8] or their combination.[8] In addition, mesoporous directing agents can be used, such as cetyltrimethylammonium bromide (CTAB),[8,13] N-phenylaminopropyltetrasiloxane,[13] dimethyloctadecyl[(trimeth-

ChemSusChem

Reviews

doi.org/10.1002/cssc.202001223

Chemistry
Europe
European Chemical
Societies Publishing

Table 3. Yield of methyl lactate over different catalysts together with the concentration of Lewis acid sites and the ratio between mesopore (V_{meso}) vs micropore volume (V_{micro}) of the catalyst.

Entry	Catalyst	Catalyst preparation method	Conditions in glucose transformation	Catalyst properties	Specific surface area [$m^2 g_{cat}^{-1}$]	Total acidity (NH$_3$ TPD) [mmol g_{cat}^{-1}]	Yield of MeLa [%]	Ref.
1	Sn-Beta-H	Sn was incorporated into delualuminated (with HNO$_3$) Beta zeolite via grinding inside a glovebox and thereafter calcined	10 bar N$_2$, 160 °C, 0.125 mol L^{-1}, glu/cat 1.4 wt/wt, 20 h, ethanol	3.7 wt% Sn, pore size up to 40 nm, average 12 nm	8.5	n.a.	52	[21]
2	deAl–Sn-BEA (100)	Post-synthesis of dealuminated zeolite, Sn loaded via incipient wetness method	160 °C, 0.14 mol L^{-1}, 3 wt% glucose in MeOH, 1 wt% catalyst, 5 h	pore size 2.2 nm, Si/Al = 102.5	592	0.071	12	[8]
3	deAl–Sn-USY-25	dealumination and Sn impregnation[55]	160 °C, 0.14 mol L^{-1}, 3 wt% glucose in MeOH, 1 wt% catalyst, 5 h	pore size 2.6 nm, Si/Al = 111.3	758	0.069	12	[8]
4	deSi-deAl Sn-BEA (100)	desilication of beta zeolite with alkali followed by acidic dealumination and Sn impregnation[56]	160 °C, 0.14 mol L^{-1}, 3 wt% glucose in MeOH, 1 wt% catalyst, 5 h	pore size 4.8 nm, Si/Al = 137.3	638	0.095	8	[8]
5	DR-deAl Sn-USY (25)	zeolite was dissolved with NH$_4$OH; reassembly was carried out with hydrothermal treatment using CTAB as a template for 48 h at 150 °C	160 °C, 0.14 mol L^{-1}, 3 wt% glucose in MeOH, 1 wt% catalyst, 5 h	pore size 3.4 nm, Si/Al = 70	626	n.a.	4	[8]
6	Sn-BEA-HT (100)	homogeneous gel was prepared from NaOH, NaAlO$_2$ in TEAOH; PDADMA was added to gel and mixed for 24 h; crystallization was performed during 1 week in autoclave at 140 °C	160 °C, 0.14 mol L^{-1}, 3 wt% glucose in MeOH, 1 wt% catalyst, 5 h	pore size 7 nm, Si/Al = 111.3	528	0.076	7	[8]
7	K–Sn-Al-USY	Sn-USY was prepared by dealumination of USY with HNO$_3$ followed by chemical grafting of SnCl$_4$·5H$_2$O in triethylamine,[48] dried and calcined at 200 °C; thereafter the catalyst was ion exchanged with 7 mol L^{-1} KCl	170 °C, 0.26 mol L^{-1}, glu/cat 2.4 wt/wt, 6 h, MW[a]	2.4 wt% Sn, molar Brønsted-to-Lewis acid ratio 0.034	n.a.	n.a.	41	[30]
8	Sn-Beta	mesoporous Sn-Beta was prepared using TEAOH as template together with TEOS; thereafter SnCl$_4$·5H$_2$O was added dropwise to this solution and stirred several hours; SiO$_2$ or Beta were used as seeds; solid gel was formed after addition of HF; zeolite crystallization was performed in oil batch at 140 °C	40 bar He, 200 °C, 0.11 mol L^{-1}, fru/cat 0.75 wt/wt, 0.5 h, water	pore size 10.6 nm	623	n.a.	58 lactic acid	[33]
9	Zr-SBA-15	In situ synthesis of SBA-15 loaded with Zr: according to Ref. [62]	27.6 bar N$_2$, 240 °C, 0.06 mol L^{-1}, glu/cat 2.0 wt/wt, 6 h	10 nm pore size	618	0.69	37	[5]
10	In-γ-Al$_2$O$_3$	In was loaded onto Al$_2$O$_3$ via wet impregnation, the material was then dried and calcined	180 °C, 0.03 mol L^{-1}, glu/cat 2.0 wt/wt, 10 h, methanol/water 13.2 v/v, addition of K$_2$CO$_3$			1.73 (NH$_3$ TPD)	34	[6]
11	Al$_2$O$_3$	Al$_2$O$_3$ was calcined at 500 °C	5 bar Ar, 160 °C, 0.06 mol L^{-1}, 6 h		209	0.16 (pyridine FTIR)	34	[14]
12	Fe$_2$O$_3$/SnO$_2$	SnCl$_4$ solution was mixed with Fe(NO$_3$)$_3$ solution under stirring; thereafter NH$_4$OH was added and pH was adjusted to 9.5; the precipitate was dried and calcined	10 bar, 160 °C, 0.06 mol L^{-1}, glu/cat 1.4 wt/wt, 20 h	pore size av. 6 nm	83	19 mL g^{-1} by NH$_3$ TPD	35	[35]

Table 3. continued								
Entry	Catalyst	Catalyst preparation method	Conditions in glucose transformation	Catalyst properties	Specific surface area [$m^2 g_{cat}^{-1}$]	Total acidity (NH$_3$ TPD) [$mmol\, g_{cat}^{-1}$]	Yield of MeLa [%]	Ref.
13	γ–NiOOH (Ni/2Hmim-4)	2-methyl-imidazole water solution was added drop-wise to a solution containing nickel nitrate and water, the precipitate was washed and dried at 100 °C under vacuum	220 °C, 0.037 mol L^{-1}, glu/cat 3.0 wt/wt, 3 h, near-critical methanol	aurface area 126 m^2 g$_{cat}^{-1}$ Brønsted-to-Lewis acid site ratio 0.1	126	0.009 µmol g$_{cat}^{-1}$	35	[11]
14	Mg-MOF-74	In situ synthesis of Mg-MOF-74 was performed via dissolving magnesium nitrate and 2,5-terepthalic acid in N,N-dimethylformamide according to Ref. [57]	220 °C, 0.037 mol L^{-1}, glu/cat 3.0 wt/wt, 3 h, near-critical methanol	specific surface area 561 m^2 g$_{cat}^{-1}$	562		26	[10]

ylsilyl)propyl]ammonium chloride,[13] diquarternary ammonium salt C$_{22-6-3}$[13] and poly(diallyldimethylammonium chloride) (PDADMAC).[7,8] One promising method is to dissolve a zeolite followed by its reassembly in the presence of CTAB.[8] Alternatively, materials with a high external surface area and mesopores, namely nanosized zeolites,[13] nanosheets[13] and delaminated zeolites[13] have been used in glucose transformation.

Dealumination of zeolites to remove aluminium, which is not affecting much textural properties of Beta zeolite,[34] is typically made with, for example, nitric[3] or oxalic acid.[7] Si/Al ratio increases sharply during dealumination of zeolite and Al can be completely removed resulting in the Si/Al ratio up to 1700.[3,4,34] It was possible to introduce Zn or Sn into a zeolite framework after dealumination.[34] As a result enhanced Lewis acidity promoted ML formation.[7]

In a two-step method, comprising first of dealumination with an acid followed by desilication with an alkali, vacant sites associated with silanols are created.[4,7] During a solid-state ion-exchange with grinding Sn-Beta with SnCl$_4$·5H$_2$O can be incorporated into the zeolite framework.[4] When silanol groups condense, Sn is incorporated into the framework sites.[4] A

special care should be taken to use dehydrated dealuminated zeolite and SnCl$_4$ under inert atmospheres to avoid formation of extra-framework metal species.[48]

Performance of dealuminated Sn zeolites was compared for dealuminated and desilicated Sn-Beta and Sn-modified USY zeolite prepared via dissolution reassembly and Sn-impregnation (noted as DR-deAl Sn-USY).[8] The authors[8] reported that dealuminated Sn-Beta-100 and Sn-USY-25 with the pore sizes of 2.2 nm and 2.6 nm, respectively (Table 3, entries 2 and 3)[8] gave higher yields of ML than the dealuminated and desilicated Sn-Beta as well as DR-deAl Sn-USY (Figure 3b, Table 3, entries 4 and 5). The two deSi-deAlSn-Beta and DR-deAl Sn-USY catalysts exhibited larger pores than only dealuminated counterparts.[8] The post synthesized catalysts contained also a large amount of silanol groups and exhibited, a lower reaction rate and ML yield.[8] Thus it was concluded,[8] that confinement of Sn into the microporous structure has a positive effect on ML yield, while in[7] the glucose transformation rate was directly correlated with the concentration of Lewis acid sites in the hierarchical Sn-Beta zeolite giving also the highest yield of ML (Table 2, entries 21–24). It should, however, be stated that in Ref. [7] the pore sizes are larger than in Ref. [8] (Table 3, entries 4 and 5).
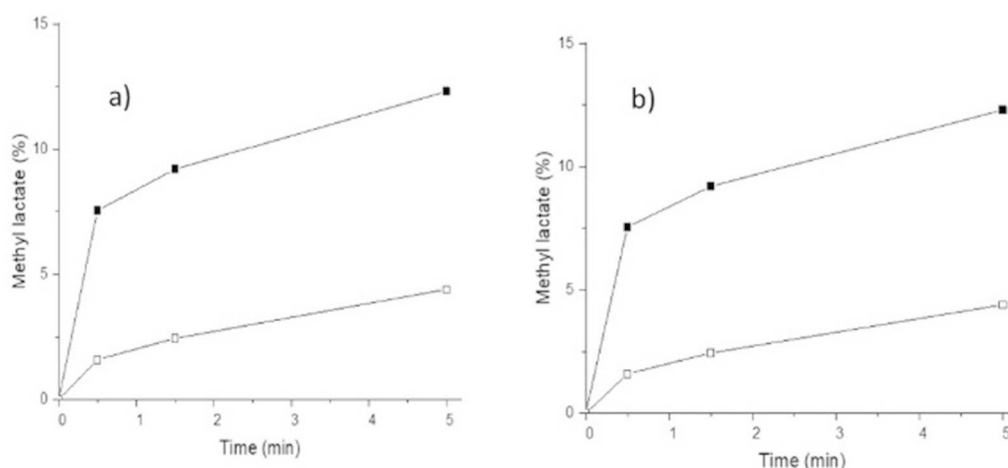

Figure 3. Yields of ML over a) dealuminated Sn-BEA (100) (■), Sn-Beta-HT (100) (●) and desilicated and dealuminated Sn-BEA(100) (□); b) dealuminated Sn-USY (25) (■) and dealuminated Sn-USY (25) prepared via dissolution-reassembly, acidic dealumination and Sn-impregnation (□) adapted from Ref. [8]. Conditions: glucose 3 wt% in methanol, 1 wt% catalyst, 160 °C in 5 h.

ChemSusChem

Reviews
doi.org/10.1002/cssc.202001223

**Chemistry
Europe**
European Chemical
Societies Publishing

Mesoporous directing agents such as PDADMAC[7] and CTAB[8] can be used in the dissolution reassembly method. For example, an increased amount of PDADMAC higher Sn loading (2 wt% and 4 wt%) and Lewis acidity were obtained giving also a higher yield of ML (Figure 4, Table 2, entries 21 and 22).[7] Furthermore, the Lewis acidity increased in the following order: Hf < Zr < Sn which apparently resulted in higher ML yields obtained with Sn-Beta-H4 (Table 2, entries 22–24) and no leaching of the catalyst occurred (see Section 4.2). On the other hand, dealuminated Sn-BEA prepared by dissolution reassembly (Table 3, entry 5) and using CTAB as a pore directing agent was less active than, for example, dealuminated Sn-BEA(100) with even smaller pore sizes.

It should, however, be pointed out that the pore size of DR-deAl–Sn-USY(25) was smaller[8] than that reported in Sn-Beta-H4 (Table 2, entry 22) indicating that even a larger pore can enhance formation of ML in Sn-Beta-H4.[7] In general it should be stated that dealuminated Sn-Beta catalyst prepared by grinding the Sn precursor with the support is quite stable in sugar transformation in methanol, while in water it suffered substantial leaching of Sn (see Section 6).[23]

Mesoporous Sn-Beta prepared by using TEOS as a template was also efficient for transforming glucose to LA at 200 °C after 30 min with the yield of 58% (Table 3, entry 8).[33] This catalyst exhibited a large pore size of 10.6 nm.

Nanostructured Sn-MFI and Sn-MWW zeolites prepared by different methods were compared in glucose transformation and related to the performance of corresponding bulk zeolites (Table 2, entries 26–36).[13] The Sn-MFI nanoparticles were prepared as described in Table 2, entry 33,[13] while delaminated Beta sheets were prepared according to a method in Ref. [49] in which the mixture containing CTAB was sonicated (Table 2, entry 31).[13] Sn-MWW nanoparticles were synthesized using dimethyloctadecyl[(trimethylsilyl)propyl]ammonium chloride as a mesopore directing agent (Table 2, entry 32).[51]
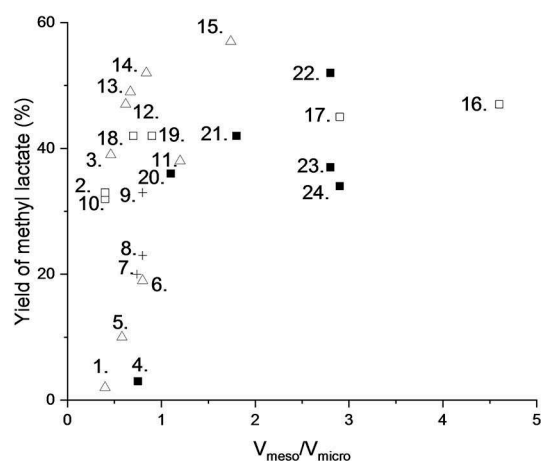
The nanostructured Sn-MWW and Sn-MFI catalysts exhibited a higher Sn loading than the corresponding bulk zeolites (Table 2, entries 33 and 34 with 29)[13] and the amount of Sn on the external surface was higher for nanostructured zeolites. The yield of ML could not be correlated either with Sn loading or with Lewis acidity.[13] In addition Sn-MFI-meso prepared via desilication and dealumination exhibited a high V_{meso}/V_{micro} ratio (Figure 2), resulting in, however, only 15% yield of ML in glucose transformations (Table 2, entry 25). The yield of ML in glucose transformations was, however, lower over bulk Sn-MOR and Sn-MWW zeolites than over mesoporous Sn-MWW nanoparticles and nanosheets (Figure 2).

Nanosized Sn-Beta, Sn-Beta nanosheet and desilicated Sn-Beta with enhanced mesoporosity and high Sn loading were used as catalysts in sugar transformations.[4] The synthesis method for nanosized Sn-Beta zeolite is described in Table 2, entry 16. Different batches were denoted as Si-Beta-xh with different crystallization times. Smaller particles were obtained (Table 2, entry 18) than with a conventional fluoride method (Table 2, entry 3).[51] The catalytic results over nanosized Sn-Beta (Table 2, entries 16–19) show that the highest yield of ML was obtained with the catalyst crystallized for 4 h (Table 2, entry 16), whereas with a longer crystallization time the V_{meso}/V_{micro} decreased, suppressing the yield of ML, even if with longer crystallization times, that is, 12 h and 24 h a lower amount of Sn could be loaded due to a more crystalline material.[4] As a comparison, Sn-Beta-AT prepared via desilication exhibited low V_{meso}/V_{micro} ratio and gave also a relatively low ML yield (Table 2, entry 10).[4] As a conclusion, it can be stated based on[4] the results with nanosized Sn-Beta catalysts exhibiting high amounts of mesopores showed clearly that catalyst morphology has also a large impact on glucose transformations.

3.2. Desired properties of metal-modified zeolites and hierarchical zeolites

Based on the experimental observations mentioned above, the most important catalyst properties for selective production of ML and LA were identified, that is, the amount of silanol groups on the catalyst surface,[1] porosity,[3,4,7,13] catalyst acidity[3,5,7] and the amount of framework metal[7] and catalyst basicity[1,34] which are discussed in more detail in this section.

A high amount of silanol groups is not desirable for transformations of sugars to alkyl lactates and LA.[1,4] The presence of such silanol groups was confirmed by TGA in post-synthesized catalysts.[7] Furthermore, a lower amount of silanols was present in 1Mg–Sn-Beta prepared by the incipient wetness method on dealuminated Al-Beta in comparison to 4Mg–Sn-Beta (Table 2, entries 39 and 40).[1] As a comparison, a post synthesized catalyst, formed after grinding SnCl4 precursor with dealuminated Beta and calcined, containing a large amount of silanol groups exhibited a lower reaction rate and the yield of ML remained constant after a short reaction time. 1Mg–Sn-Beta[1] was a slightly more efficient catalyst to produce ML with the yield of 46% in comparison to 42% over 4Mg–Sn-Beta (Table 2, entry 39 and 40) with a higher amount of silanols. An

Figure 4. Correlation between methyl lactate yield and ratio between meso- and micropore volume. Data is taken from Ref. [7] for mesoporous catalysts (■) and from Refs. [7] (+), [4] (□) and [3] (▲) for microporous catalysts. Notation: numbers are given in Table 1. Reaction conditions: 0.014 mol L⁻¹ glucose in methanol, glu/cat 1.6 wt%/wt%, 160 °C, 10 h [3, 4] 0.14 mol L⁻¹ glucose in methanol, glu/cat 1.6 wt%/wt%, 160 °C, 6 h adapted from Ref. [7].

ChemSusChem

Reviews
doi.org/10.1002/cssc.202001223

Chemistry
Europe
European Chemical
Societies Publishing

explanation is the formation of MgO clusters with a higher amount of Mg, thus not interacting with silanols.

Catalyst acidity and basicity[1] is of great importance in sugar transformations. Typically, hierarchical Sn-Beta zeolites contain no or very small amounts of Brønsted acidity,[7] while Lewis acidity is enhanced due to presence of Sn in the framework position.[4,7] When silanol groups condense, Sn is incorporated into the framework sites. Al content typically decreases during dealumination of zeolites[13,34] influencing negatively the Brønsted acidity of hierarchical zeolites. An interesting observation was reported in Ref. [1] namely that the Lewis acidity of 4Mg–Sn-Beta was higher than for 1Mg–Sn-Beta, still generating less ML. In[1] basicity of different catalysts was investigated by FTIR spectra of adsorbed $CHCl_3$ revealing that 4MgSn-Beta exhibited also the highest basicity. This catalyst gave a slightly lower ML yield in comparison to 1MgSn-Beta (Table 2, entries 39 and 40).[1] Thus, it was concluded that high basicity is not desired. An opposite result was obtained in glucose transformations to LA over Zn–Sn-Beta, which has also some basicity. It was claimed in Ref. [34] that the presence of basic sites, determined in that work by CO_2 temperature programmed desorption, inhibits transformation of fructose to HMF.

The metal location in zeolites and its quantity are important for achieving high yields of the desired product. Isolated Sn species can be incorporated in the framework position of dealuminated Al-Beta containing vacant T sites[1] via the solid state ion-exchange giving framework Sn^{4+} species with Lewis acidity. The framework location of metal can be confirmed by several methods, that is, XRD,[34] Raman spectroscopy,[34] FTIR of CH_3CN[4] and XPS.[4] XRD results should confirm an increased lattice spacing in the d_{302}, because the ionic radii of Sn and Zn are bigger than that of Al. Furthermore, framework Sn is present as metallic species based on the Raman spectra[34] or XPS,[4] while extra-framework metal species are oxides. For example, in Ref. [7] it was shown that Sn^{4+} was in framework position, while octahedrally coordinated SnO_2 was present in Si-Beta.[4] Si-Beta contained SnO_2 located in a non-framework position and gave only 4% yield of ML, while not surprisingly Sn-Beta-9 h catalyst was much more efficient to ML with 43% yield (Table 2, entry 18).[4] It was also stated in Ref. [7] that TEM is a suitable method to reveal if Sn is in the framework, that is, the d spacing in Beta is increased after Sn incorporation in its framework as the ionic radius of Sn is larger than that of Si, being 1.063 and 1.089 nm, respectively.[7] Another method to study the presence of Sn framework species is FTIR spectra of CH_3CN giving absorbance at 2310 cm^{-1}.[4] In addition Sn-Beta-150 HT, which afforded 47% ML in 12 h at 160 °C[9] (Table 2, entry 27b).[9] These results show clearly the importance of framework Sn^{4+} species, elevating Lewis acidity of the catalyst. Location of Sn can be compared using XPS giving the amount of surface species and ICP analysis, reflecting the bulk content.[54] For conventional zeolites, Si/Sn ratio in the catalysts prepared by hydrothermal method using HF[53] was typically lower than for Sn supported on MFI zeolites, because dealumination was more efficient for large pore MOR and Beta zeolites, while for MWW and MFI it was only 57% and 32%, respectively.[13]

Textural properties can affect sugar transformation to alkyl lactates, for example, nanosized Sn-Beta-4 h zeolite (Table 2, entry 16) containing no Brønsted acid sites was active in glucose transformation at 160 °C producing 47% ML after 10 h.[4] This catalyst contained a large amount of mesopores because of nano size particles facilitating better accessibility of glucose to interact with the active sites.[4] When the ML yield in glucose transformations is depicted as a function of the ratio between the mesopore to micropore volumes of different catalysts based on data presented in[3,4,7] (Figure 4), the ML yield was the highest over mesoporous Sn-Beta-H-0.4 which contained a large amount of structure directing agent TEAOH (Table 2, entry 15)[3] and exhibited the V_{meso}/V_{micro} ratio of 1.74. The lowest ML yields were obtained with microporous Al-Beta (Table 2, entry 1)[3] and with a non-acidic Si-Beta catalyst. It was also interesting to observe that for V_{meso}/V_{micro} ratio of 2.8–2.9 the yield of ML increased up to the Lewis acidity value of 54 mmol g$_{cat}$$^{-1}$, decreasing beyond this value (Table 2, entries in Figure 4). On the other hand, microporous Sn-Beta-P, Hf-Beta and Zr-Beta gave only relatively low ML yields (19–23%, Table 2, entries 6–8 in Figure 4). A comparative work with a microporous Sn-Beta-F and hierarchical Sn-Beta-0.3 was also made for fructose in addition to glucose transformations (Table 2, entries 3 and 14).[3] It was stated in Ref. [3] that for both cases a higher yield of ML (58%) was obtained with the hierarchical Sn-Beta-0.3, although these two catalysts exhibited the same crystal sizes, acidities and Sn content. Thus it was concluded that the only reason for a better performance of hierarchical Sn-Beta-0.3 was the presence of hierarchical pores.[3] This catalyst suffered from fouling but could be regenerated via calcination (see Section 4.2). Over Sn-MOR-bulk catalyst with high Lewis and Brønsted acidity, only 20% yield of ML was obtained in 20 h (Table 2, entry 28) (Figure 2).[13]

3.3. Non zeolitic catalysts for transformation of glucose to alkyl lactate

Mixed oxides containing different amounts of Fe_2O_3 and SnO_2 were prepared by adding neat SnO_2 nanocrystals into an aqueous solution of Fe_2O_3, adjusting the pH and calcining. The best performing catalysts, with 0.2 Fe_2O_3 in SnO_2 (in which 0.2 denotes Fe/(Fe + Sn) molar ratio) when Fe^{3+} was inserted into the SnO_2 crystal lattice,[35] gave the highest yield of ML due to a high Lewis acidity of this catalyst (Table 3, entry 12).

Several metals, such as Ni, Zn, Co and Mg bound with metal organic framework were tested in glucose transformations to ML. Mg-MOF-74 exhibiting also the highest specific surface area was the best one (Table 3, entry 14).[10] Metal organic frameworks are known to exhibit high thermal stability, ordered structures allowing a high metal content in it.[58]

Several metal oxides (Al_2O_3, TiO_2 and ZrO_2) were investigated in glucose transformation to ML.[14] The most promising catalyst exhibiting both high amounts of acid and base sites was γ-Al_2O_3 calcined at 500 °C giving 34% ML yield at 160 °C after 6 h (Table 3, entry 11). As a comparison the yields of ML were for Al_2O_3 and TiO_2 34% and 10%, respectively.[14] In-

ChemSusChem

Reviews
doi.org/10.1002/cssc.202001223

**Chemistry
Europe**
European Chemical
Societies Publishing

modified γ-Al$_2$O$_3$ with different In loading was also investigated in glucose transformations. An optimized In loading (12 wt%) facilitated the highest total acidity[6] and 34% yield of ML at 180°C in 10 h (Table 3, entry 10).[6] Uniformly dispersed In with the size of 20–25 nm was present on Al$_2$O$_3$ as In$_2$O$_3$.

The effect of the pore size of Zr-SBA-15 was systematically investigated in xylose transformation to ML at 240°C.[5] Less furfural and humins were formed with increasing the pore size of the catalyst, that is, with 7 nm and 10.6 nm pores, 17% and 6.9% solid residue, respectively, was formed.

An optimum Lewis acid site concentration in γ–NiOOH (Ni/Hmim) with the highest specific surface area among different γ–NiOOH (Ni/Hmim) catalysts facilitated the highest ML yield, (Table 3, entry 13) due to better accessibility of glucose to active sites of the catalyst.[11] As a conclusion it can be stated that an active and selective catalyst for glucose transformation to ML should have strong Lewis acidity and the presence of framework metal species. Post synthesis methods, such as dealumination create vacant sites in the framework, allowing high metal loading in the framework while the hierarchical channel system suppresses diffusional limitations.

4. Reaction Conditions for Sugar Transformation to Alkyl Lactates and Lactic Acid

4.1. Effect of reaction conditions

For hierarchical Sn-Beta-H4 zeolite the ML yield increased with increasing temperature and the highest yield was obtained at 180°C (Figure 5a).[7] On the other hand, it was observed in several studies that Sn-modified catalysts gave the highest ML yield in glucose transformation at 160°C[18,35] For 1Mg–Sn-Beta catalyst 170°C was found as an optimum temperature for glucose transformations to ML.[1] A slightly higher optimum temperature, 180°C was observed for ML yield over γ–NiOOH

(Ni/2-Hmim).[11] The optimum temperature in fructose transformations to ML over Sn(salen)/IL catalyst was also 160°C.[18]

An optimum temperature for glucose transformation to LA over Sn-Beta catalyst was 200°C giving the highest yield of LA after 30 min reaction time under 40 bar.[33] A higher reaction temperature can also be advantageous for carbohydrate transformations because of a larger fraction of a more reactive acyclic form confirmed by DFT calculations.[13] The acyclic form can facilitate carbohydrate transformations in the micropores of MWW imposing less severe steric hindrance in comparison to the cyclic form.

For glucose transformations over hierarchical Sn-Beta-zeolites it was shown that the activation energy for glucose transformations is in the range of 96–100 kJ mol^{-1}.[3] Sn-Beta catalyst exhibited 39% higher activation energy in fructose transformations to ML in comparison to 1Mg–Sn-Beta.[1] The activation energy for ML formation from 1,3-dihydroxyacetone and from fructose was determined in Ref. [18], being 46.4 kJ mol^{-1} and 71.5 kJ mol^{-1}, respectively, showing that the latter reaction is a more demanding one.

The effect of helium pressure was investigated in glucose transformations to LA between 1–60 bar at 200°C over a hierarchical Sn-Beta catalyst. The results revealed that LA formation was the highest under 40 bar of helium due to presence of subcritical water.[33] On the other hand, opposite results were obtained in glucose transformations to ML over hierarchical Sn-Beta-H4,[7] when the best ML yield (44%) was achieved under 5 bar nitrogen, while at 40 bar only 32% yield of ML yield was obtained (Figure 5b).

Typically, methanol, ethanol,[3,21] n-butanol[3,21] and water[5,9,33,34] or combination of water and methanol[9,23] have been used as solvents in sugar transformations. Lower yields of alkyl lactates have been obtained in ethanol and n-butanol in comparison to methanol due to the presence of longer carbon chain alcohols.[3,21] Noteworthy is that when changing methanol to water as a solvent in xylose transformation over Zr-SBA-15 at 240°C, the yield of ML was 37% (Table 1, entry 22), while the LA yield was only 6%.[5] It was stated in,[5] that the reason for a low
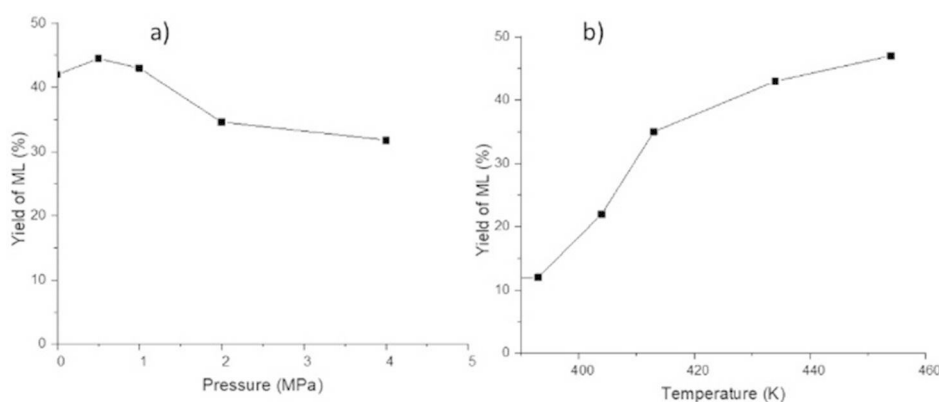

Figure 5. Effect of a) reaction temperature and b) pressure in glucose transformation over Sn-Beta-H4 at a) 5 bar N$_2$ and b) 160°C. Conditions: 0.137 mol L^{-1}, glu/cat 1.6 wt%/wt%, 6 h adapted from Ref. [7].

ChemSusChem

Reviews
doi.org/10.1002/cssc.202001223

Chemistry
Europe
European Chemical
Societies Publishing

LA yield in water is a change of the Lewis acid sites in Zr-SBA-15 to Brønsted ones.

Effect of water in glucose transformation to ML was also investigated[9] and the final ML yield in the presence of 2–10% water in methanol was approximately the same as the ML yield after 240 min at 160 °C over hydrothermally prepared Sn-Beta, while in the absence of water a slightly higher ML yield was obtained. It was additionally pointed out that the presence of water favours formation of carbonaceous species and Brønsted acid catalysed species.[25]

Complete glucose conversion in glucose transformations at 160 °C over Fe_2O_3/SnO_2 was obtained in 20 h with different glucose concentrations up to 0.06 mol L^{-1}. Unfortunately, kinetic data for different initial glucose concentrations were not shown.[35] At the same time, the ML yield increased after 20 h with increasing initial glucose concentration up to 0.05 mol L^{-1} remaining constant thereafter due to slightly increasing amounts of pyruvaldehyde dimethylacetal.[35] In Ref. [1] the yield of ML after 5 h, however, slightly decreased with increasing the initial glucose concentration from 0.137 mol L^{-1} to 0.55 mol L^{-1} at 170 °C over 1Mg–Sn-Beta catalysts. In the absence of kinetic data for different initial glucose concentrations assessment of the reaction order to glucose is difficult.

Complete conversion of fructose was obtained after 2 h at 160 °C under 20 bar in its transformations over Sn(salen)/IL catalyst, when varying the initial fructose concentration from 0.04 to 0.18 mol L^{-1}. The yield of ML was the highest using 0.11 mol L^{-1} initial fructose concentration, that is, increasing from 55% yield to 68% in the concentration range 0.04 mol L^{-1} to 0.11 mol L^{-1} decreasing thereafter to 60%.[18]

ML yield increased with increasing catalyst loading in glucose transformations at 240 °C over Zr-SBA-15[5] and at the same time the yield of glycolaldehyde dimethylacetal and methyl glycolate decreased. ML yield increased also in glucose transformation at 200 °C over γ–NiOOH (Ni/2-Hmim) catalyst up to 0.2 g of catalyst whereas with higher catalyst amounts the yield remained constant.[11] On the other hand, in fructose transformations complete conversion was obtained in 2 h. At the same time, the yield of ML increased with increasing NiOOH catalyst amounts in fructose transformations to ML at 200 °C,[12] while an optimum catalyst loading was observed in this reaction over Sn(salen)/IL at 160 °C. For higher catalyst amounts the yield of ML even decreased.[18] In their case[18] the sum of the product yields decreased. It should be stated here that kinetics for fructose transformation was not studied with different catalyst masses and thus a comprehensive kinetic analysis based on the available data[18] is not possible.

4.2. Catalyst stability, deactivation, regeneration and reuse

Possible leaching of the metals has been investigated both in water[34] and in methanol[7] showing robustness of catalysts in both media. In glucose transformation performed in water[34] and methanol[7] the hot filtration test results showed that both LA yield over Zn–Sn-Beta at 190 °C and ML yield Sn-Beta-H4 at 160 °C remained constant after filtering the catalyst away.[7]

Catalyst recyclability has been intensively studied both in sugar transformations to ML[3,4,7,21,30] and LA.[33,34] Typically, nearly the same ML yield was obtained in glucose transformation over Sn-Beta catalysts at 160 °C under 5 bar nitrogen with 0.14 mol L^{-1} initial glucose concentration, that is, 48% yield in the first and 47% yield of ML in the fifth experiment.[4] The catalyst was regenerated between each experiment via washing with methanol, drying and calcination at 550 °C for 5 h.[4] Analogously Sn-Beta-H-0.3 catalyst was stable in five consecutive experiments in glucose transformation at 160 °C to ML,[3] when the catalyst was treated at 160 °C in methanol for 10 h, after which it was washed, dried and calcined at 550 °C for 6 h. More stable catalysts should be developed for sugar transformations in water.[34] Typically, high temperature calcination in air is required for hierarchical Sn-Beta and K–Sn-Al-USY catalysts.[7,21,30,33] The conversion decreased over 1MgSn-Beta catalyst in five consecutive experiments from 78% to 76% at 120 °C, while only less than 3% of Sn and Mg were leached.[1] Sn(salen)/IL catalyst was successfully recycled giving the same ML yield in glucose transformations, when the catalyst was washed with ethyl acetate between experiments.[18] Noteworthy is that only washing the spent Fe_2O_3/SnO_2 catalyst with methanol and drying at 100 °C facilitated its successful reuse in glucose transformations.[35]

Catalyst recyclability in water was much worse compared to methanol.[34] For example Zn–Sn-Beta catalyst gave only 12% yield of LA in the fifth consecutive experiment, while it was 47% in the first one in glucose transformations at 190 °C. The catalyst was regenerated in static air at 550 °C for 6 h. It was also speculated that catalyst deactivation is related e to metal leaching.

For recycling of Zr-SBA-15 catalyst used in xylose transformations at 240 °C, only drying in an oven between the experiments was performed.[5] It turned out that ca. 10% of the solid residue was collected on the outer surface of the catalysts in line with just a slight decrease of the ML yield. In addition, recyclability of In/Al$_2$O$_3$ was rather good in glucose transformations to ML with only minor leaching observed after the first run.[6] Analogous results were also obtained for Mg-MOF-74 when the catalyst was only dried in vacuum at 100 °C overnight.[10] Recyclability test of NiO catalyst gave a lower ML yield in fructose transformations in consecutive experiments due to encapsulation of NiO with a carbonaceous material[12] whereas the yield of ML in glucose transformations decreased also slightly over γ–NiOOH (Ni/2-Hmim). The latter catalyst was soaked in methanol and dried in vacuum at 100 °C between the experiments.[11] The phase composition of the catalyst was however, kept intact, which was confirmed by XRD.[11]

As a conclusion, it can be stated that the optimum temperature, feed concentration and catalyst amounts have been determined in glucose and fructose transformations. Since kinetics has not been comprehensively studied, that is, investigating initial transformation rates of the reactant at different amounts of catalyst, initial feedstock concentrations, pressures and temperatures, their effect cannot be fully assessed. Several catalysts have shown excellent recyclability

ChemSusChem

Reviews
doi.org/10.1002/cssc.202001223

**Chemistry
Europe**
European Chemical
Societies Publishing

and in some cases catalyst regeneration by calcination was required.

5. Kinetic Regularities and Kinetic Modelling for Sugar Transformations to Alkyl Lactate and Lactic Acid

Kinetics of 1,3-dihydroxyacetone[16] and sugar transformations to alkyl lactates[9,18] and LA[33,34] has been quite scarcely investigated. 1,3-Dihydroxyacetone was transformed to ethyl lactate for example over a Lewis acidic Sn/Al$_2$O$_3$.[16] Conversion of 1,3-dihydroxyacetone was close to 100% already at 80 °C in 7 h in a batch reactor giving ethyl lactate and glyceraldehyde diethyl acetal as the main products (Figure 6).

In addition, pyruvaldehyde reacted further to pyruvaldehyde hemiacetal and ethyl lactate after 1.6 h after, while a part of pyruvaldehyde hemiacetal was also transformed to pyruvaldehyde diethylacetal. Glyceraldehyde diethyl aldehyde could also be formed parallelly from 1,3-dihydroxyacetone. Several kinetic models were developed for DHA transformation to ethyl lactate and the model describing the experimental data in the best way comprised the following rate equations:

$$r_2 = k_2 c_{DHA} \tag{1}$$

$$r_4 = k_4^* c_{PA} - k_{-4} c_{PAHA} \tag{2}$$

$$r_5 = k_5^* c_{PAHA} \tag{3}$$

$$r_6 = k_6 c_{PAHA} \tag{4}$$

$$r_7 = k_7^* c_{DHA} - k_{-7}^* c_{GLADA} \tag{5}$$

$$r_8 = k_8 c_{DHA} - k_{-8} c_{others} \tag{6}$$

In which k_4^*, k_5^* and k_6^* are defined as:

$$k_4^* = k_4 c_{EtOH4}^0 \tag{7}$$

$$k_5^* = k_5 c_{EtOH5}^0 \tag{8}$$

$$k_7^* = k_7 c_{EtOH7}^0 \tag{9}$$

Notation of steps is presented in Figure 7. Concentration c_i denotes reactant and product concentrations at time t, while c_{EtOH}^0 reflects the initial concentration of ethanol. According to this model ethyl lactate is mainly formed from pyruvaldehyde hemiacetal, while 1,3-dihydroxyacetone reacts also reversibly to glyceraldehyde diethylacetal and other compounds.

Furthermore, a minor part of pyruvaldehyde hemiacetal reacts also irreversibly to pyruvaldehyde diethyl acetal (Figure 7). The description of the data was adequate with the goodness of the fit reaching ca. 97%.

A comparative kinetic study of the transformations of sucrose, glucose and fructose over HT Sn-Beta (150) catalyst at 160 °C showed that the ratio between the initial transformation rates of sucrose/glucose/fructose during 0–30 s was 8.7:3.3:1, that is, a dimer reacts much slower than glucose and fructose (Figure 8).[9] Furthermore, in Ref. [9] formation of methyl fructosides (Figure 9) from fructose during the first 10 min of the
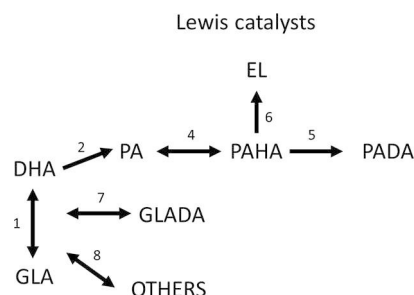
Figure 7. Simplified reaction scheme for transformation of 1,3-dihydroxyacetone to ethyl lactate based on a kinetic model adapted from Ref. [16].

Figure 6. Transformation of 1,3-dihydroxyacetone over Sn/Al$_2$O$_3$ as catalyst at 80 °C under 250 kPa to different products in ethanol as a solvent. Notation: 1,3-dihydroxyacetone (DHA), ethyl lactate (EL), glyceraldehyde diethyl acetal (GLADA), pyruvaldehyde (PA), pyruvaldehyde hemiacetal (PAHA), and pyruvaldehyde diethyl acetal (PADA).[16] Copyright received from Elsevier.
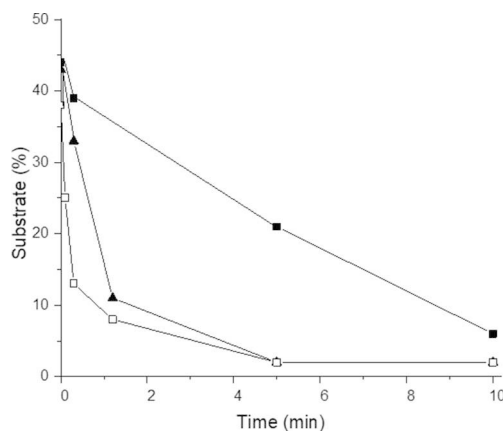
Figure 8. Amounts of sucrose (■), glucose (▲) and fructose (□) as a function of time in their transformation to methyl lactate at 160 °C over HT Sn-Beta catalyst adapted from Ref. [9].
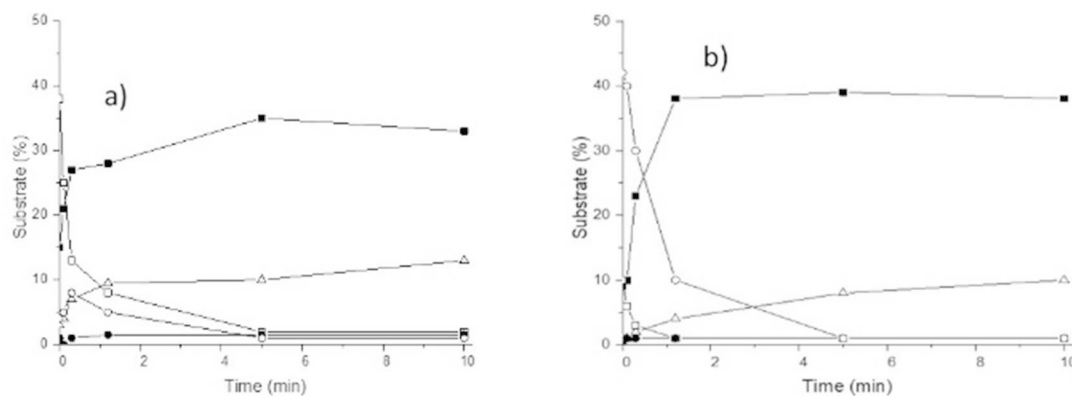
Figure 9. Amounts of reactant and products as a function of time in a) fructose and b) glucose transformation to fructose at 160 °C over HT Sn-Beta catalyst adapted from [9]. Notation: Fructose (□), methyl fructoside (■), glucose (o), methyl glucoside (●), and methyl lactate (Δ).

reaction was rapid reaching a maximum after 5 min. Thereafter, methylfructoside reacted consecutively giving the final yield of ML 47% at 720 min (Table 2, entry 27b), while methylglucoside concentration remained constant with increasing time form 60 to 240 min. Only when using 75% water-methanol mixture as a solvent it was possible to recover glucose from methylglucoside.

Kinetic modelling of ML formation was based on the first order kinetics in which glucose reacts reversibly to fructose, which in turn can reversibly form methyl fructoside. The kinetic equations in transformations of glucose were:

$$\frac{dc_{GL}}{dt} = -k_1 c_{GL} + -k_{-1} c_{FR} \tag{10}$$

$$\frac{dc_{FR}}{dt} = k_1 c_{GL} + -k_{-1} c_{FR} - k_2 c_{FR} + k_{-2} c_{Me-FR} - k_3 c_{FR} \tag{11}$$

$$\frac{dc_{Me-FR}}{dt} = k_2 c_{FR} - k_{-2} c_{Me-FR} \tag{12}$$

$$\frac{dc_{Me--Lac}}{dt} = k_3 c_{FR} \tag{13}$$

in which c_{GL}, c_{FR} and c_{Me-FR} denote concentrations of glucose, fructose and methyl fructoside, respectively. It should, however, be commented, that the proposed reaction scheme is still rather simplified, not reporting kinetic profiles for intermediates, such as pyruvaldehyde or glyceraldehyde.

In the kinetic profile for fructose transformation over Sn (salen)/IL (IL is octylmethyl imidazolium bromide)[18] fructose conversion was 100% between 0–4 h and it was clearly visible that both ML, 5-methoxymethylfurfural and pyruvaldehyde dimethylacetal concentrations exhibited a maximum after 2 h reaction time while methyl glycolate and methyl levulinate concentrations increased with increasing time (Figure 10, Table 1, entry 24). Furthermore, it was also concluded that the retro aldol splitting is the rate limiting step in fructose transformations to ML,[18] which is in line with the activation energies
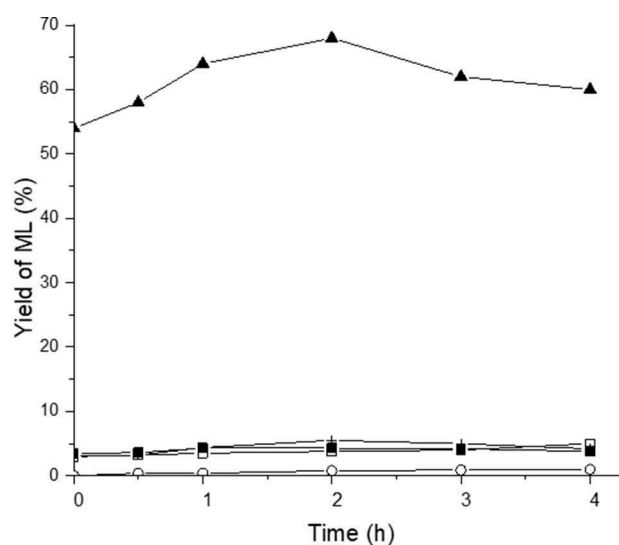

Figure 10. Kinetics in fructose transformation to ML over Sn(Salen)IL catalyst at 160 °C under 20 bar nitrogen using 0.03 mol L⁻¹ fructose in methanol; adapted from Ref. [18]. Notation: (▲) methyl lactate, (□) methyl levulinate, (+) 5-methoxy-methylfurfural, (■) pyruvaldehyde dimethylacetal and (o) methyl glycolate.

for ML formation from 1,3-dihydroxyacetone and from fructose, being 46.4 kJ mol⁻¹ and 71.5 kJ mol⁻¹, respectively, showing that the latter reaction is more kinetically demanding.

Kinetics of glucose transformations to ML was studied at 120 °C under 4 bar nitrogen showing that the main product was ML over Mg–Sn-Beta catalyst. The second highest products were trioses while also traces of LA, erythrose and mannose were formed.[1] A nearly complete conversion of glucose after 120 min with 0.37 g of catalyst.[1] Unfortunately different catalyst masses were not studied in their work[1] and thus it is not possible to make a comprehensive kinetic analysis of, for example, glucose reaction order. In the kinetic analysis[1] it was stated that the transformations of C₃ compounds backwards to ML are difficult similar to Ref. [46]. The sum of the concentration of all products gave the mass balance closure of ca. 83%.[1]

ChemSusChem

Reviews
doi.org/10.1002/cssc.202001223

Chemistry Europe
European Chemical
Societies Publishing

Glucose transformation to LA was investigated at 200 °C under 40 bar over Sn-Beta catalyst.[33] The results showed that LA yield exhibited a maximum at 30 min being 56%, after which it decreased to 45% indicating clearly that further transformations of LA are possible under these conditions. The minor products were xylitol, levulinic acid and HMF. In Ref. [34] glucose was transformed to LA at 160 °C over Zn—Sn-Beta and the total organic carbon decreased after 2 h to 80%. The main product was LA, followed by HMF, furfural and its derivatives and levulinic acid. Trace amounts of formic and acetic acids and acetol were also formed (Table 1, entry 21).

6. Continuous Reactor Operation

Continuous reactor operation has been very scarcely investigated in sugar transformations. In[23] fructose transformations to ML over dealuminated Sn-Beta was investigated in a fixed bed reactor with the time-on-stream behaviour of fructose conversion and ML selectivity shown in Figure 11.[23] The conversion declined from 88% to 63% in 100 h. The original activity of the catalyst was restored by calcination of the catalyst ex situ at 550 °C in air for 6 h. The catalyst was not, however, stable in the continuous experiments, because after 6 reaction cycles, that is, 560 h, ca. 60% of Sn was lost. Interestingly, selectivity to ML increased from 51% to 73% after the fourth cycle. When, however, 1 wt% water was fed together with methanol into the reactor, both activity and selectivity to ML were more stable. It was observed[23] that up to 5 wt% water is beneficial in fructose transformation, while if more than 5 wt% water was added into the feed, both conversion and ML selectivity decreased. It can be thus speculated that water addition can remove coke and catalyst poisons in situ. Based on TPD-MS and TGA measurements it was confirmed that both the spent catalyst in methanol as well as in water contained substantial amounts of organic compounds, which were removed during TGA measurement.
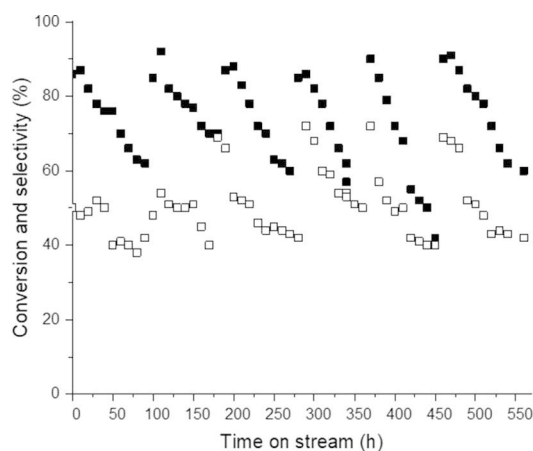
7. Reaction Mechanism for Sugar Transformations to Alkyl Lactates and Lactic Acid

Reaction mechanism for glucose transformations to ML has been extensively discussed.[6,9,18,35] In the first step is catalysed by Lewis acid sites glucose is isomerized to fructose. The carbonyl group in fructose can interact with the Lewis acidic site of, for example, Zr and at the same time OH group at the C4 carbon atom adsorbs onto oxygen atom on the base site.[59] Thereafter the C3—C4 bond in fructose is cleaved via a retro-aldol reaction forming 1,3-dihydroxyacetone and glyceraldehyde over Lewis acid sites or with a base.[14,59] 1,3-Dihydroxyacetone can in turn be tautomerized via a keto-enol mechanism including formation of enediol to glyceraldehyde (Figure 12).[59]

Puryvaldehyde is formed via Lewis acid catalysed dehydration of 1,3-dihydroxyacetone[14] or glyceraldehyde.[18] Finally, ML is formed from pyruvaldehyde via its hydration and internal Cannizzaro reaction or 1,2-shift followed by esterification with methanol.[17,18] In Ref. [18] it was stated that pyruvaldehyde reacts further to hemiacetal, which undergoes 1,2-H transfer and esterification with methanol forming ML. If Brønsted acidity of the catalyst is too high, pyruvic aldehyde dimethyl acetal, HMF and 5-(methoxymethyl)-2-furaldehyde (MMF) can be formed. In addition, it was stated in Ref. [59] that even too high base site concentration of Al_2O_3 in comparison with ZrO_2 catalysed formation of HMF. Methyl levulinate is formed as a final product from MMF through cleavage of formic acid and addition of two moles of water. Too high Brønsted acidity catalyses also formation of methylglucosides[11] and -fructosides.[9] Especially post-synthesized Sn-Beta catalyst produced more methyl glucosides due to its higher acidity in comparison to hydrothermally prepared Sn-Beta.[9] Lewis acids catalyse also retro-aldol condensation of glucose to a minor extent forming erythrose along with glycolaldehyde. Since glycolaldehyde is very unstable, it reacts rapidly with methanol forming methyl glycolate.[18] In general the liquid phase mass balance closure in sugar transformation to ML in methanol or to
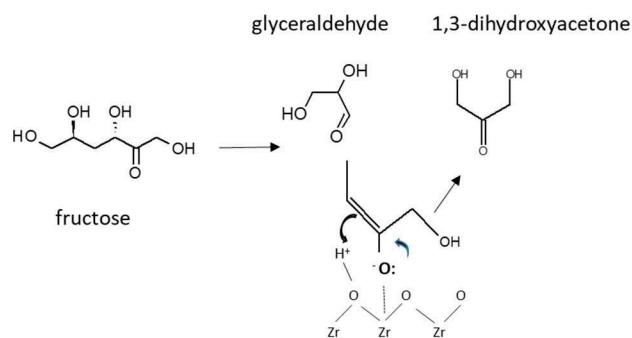

Figure 11. Fructose transformation in a fixed bed reactor as a function of time-on-stream The catalyst was regenerated ex situ at 550 °C for 6 h, adapted from Ref. [23].

Figure 12. Fructose transformation to glyceraldehyde and 1,3-dihydroxyacetone via the retro-aldol reaction on acid and base sites of ZrO_2 (adapted from Ref. [59]).

LA in water was lower than 100% indicating also formation of humins (Figure 1a).

8. Future Research Needs

Several future research needs can be clearly identified based on the analysis of literature including lack of information on a proper product analysis, which limits availability of reliable data, that is, conversion of sugars and complete product analysis including the mass balance closure. Only a few papers reported kinetic profiles for formation of several products in sugar transformations,[9,11,18] while other report only ML or LA yield and conversion.[1,4,13] Some methods, for example, 2D NMR spectroscopy, especially ^{1}H–^{13}C heteronuclear single quantum coherence (HSQC) and ^{1}H NMR spectroscopy[34] are good tools for analysis of reaction mixtures.[9,34] On the other hand, non-volatile sugars can be analysed by HPLC[3] and analysis of the products by gas chromatography combined with mass spectrometry is reliable. The GC analysis is limited by the presence of sugars, which should be separated from other products by extraction[34] or derivatization of the components.[34,60,61] Unfortunately analytical details are typically not at all discussed in many publications[11] reporting only the ML yield as a function of time.[7,10] Direct GC analysis of the reaction mixture after reaching complete conversion is possible, but this method is not revealing kinetic concentration profiles of all components. Process feasibility in terms of incomplete mass balance closure, catalyst leaching and recycling in water is still unsolved and requires further research.

9. Summary and Outlook

Recent developments in catalytic transformations of sugars to lactic acid and methyl lactate have been summarized. The highest yields of methyl lactate and lactic acid in glucose transformation under optimum conditions, 160 °C in methanol and 200 °C in water, are ca. 58% and 68%, respectively, over Lewis-acidic hierarchical Sn-modified zeolites and Sn(salen)/octylmethyl imidazolium bromide. Several challenges in sugar transformations have been identified, for example, a lack of liquid mass balance closure and presence of side reactions, such as acetalization in methanol and humin formation in water, occurring especially over highly Brønsted-acidic catalysts. A catalyst should typically be calcined at a high temperature prior to its reuse. Despite of intensive research efforts in this area, there is still a lack of proper kinetic data, in particular because of complicated analytics, which is typically not discussed in sufficient detail. Application of continuous operation for sugar transformations to the desired products has revealed occurrence of catalyst leaching, especially in water. Preliminary attempts of kinetic modelling based on a simplified reaction network were reported, but more research is required both in catalyst development, kinetic analysis and modelling.

Conflict of Interest

The authors declare no conflict of interest.

[1] X. Yang, B. Lv, T. Lu, Y. Su, L. Zhou, *Catal. Sci. Technol.* **2020**, *10*, 700–709.
[2] X. Yang, L. Wu, Z. Wang, J. Bian, T. Lu, L. Zhou, C. Chen, J. Xu, *Catal. Sci. Technol.* **2016**, *6*, 1757–1763.
[3] X. M. Yang, J. J. Bian, J. H. Huang, W. W. Xin, T. L. Lu, C. Chen, Y. L. Su, L. P. Zhou, F. Wang, J. Xu, *Green Chem.* **2017**, *19*, 692–701.
[4] X. M. Yang, Y. Liu, X. X. Li, J. X. Ren, L. P. Zhou, T. L. Lu, Y. L. Su, *ACS Sustainable Chem. Eng.* **2018**, *6*, 8256–8265.
[5] L. Yang, X. Yang, E. Tian, V. Vattipalli, W. Fan, H. Lin, *J. Catal.* **2016**, *333*, 207–216.
[6] Y. Xiao, S. Xu, W. Zhang, J. Li, C. Hu, *Catal. Today* **2020**, https://doi.org/10.1016/j.cattod.2020.02.038.
[7] B. Tang, S. Li, W. C. Song, E. C. Yang, X. J. Zhao, N. Guan, L. Li, *ACS Sustainable Chem. Eng.* **2020** 8, 3796–3808.
[8] I. Tosi, A. Sacchetti, J. S. Martinez-Espin, S. Meier, A. Riisager, *Top. Catal.* **2019**, *62*, 628–638.
[9] I. Tosi, A. Riisager, E. Taarning, P. R. Jensen, S. Meier, *Catal. Sci. Technol.* **2018**, *8*, 2137–2145.
[10] X. Lu, L. Wang, X. Lu, *Catal. Commun.* **2018**, *110*, 23–27.
[11] X. Lyu, L. Wang, X. Chen, L. Xu, J. Wang, S. Deng, X. Lu, *Ind. Eng. Chem. Res.* **2019**, *58*, 3659–3665.
[12] X. Lyu, L. Xu, J. Wang, X. Lu, *Catal. Commun.* **2019**, *119*, 46–50.
[13] W. N. van der Graaff, C. H. Tempelman, E. A. Pidko, E. J. Hensen, *Catal. Sci. Technol.* **2017**, *7*, 3151–3162.
[14] S. Yamaguchi, M. Yabushita, M. Kim, J. Hirayama, K. Motokura, A. Fukuoka, K. Nakajima, *ACS Sustainable Chem. Eng.* **2018**, *6*, 8113–8117.
[15] M. S. Holm, Y. J. Pagán-Torres, S. Saravanamurugan, A. Riisager, J. A. Dumesic, E. Taarning, *Green Chem.* **2012**, 14, 702–706.
[16] E. A. Pighin, J. I. Di Cosimo, K. Diez, *Molec. Catal.* **2018**, *458*, 189–197.
[17] D. Verma, R. Insyani, Y. W. Suh, S. M. Kim, S. K. Kim, J. Kim, *Green Chem.* **2017**, *19*, 1969–1982.
[18] F. Wang, Y. Wen, Y. Fang, H. Ji, *ChemCatChem,***2018**, *10*, 4154–4161.
[19] Q. Guo, F. T. Fan, E. A. Pidko, W. N. P. van der Graaff, Z. C. Feng, C. Li, E. J. M. Hensen, *ChemSusChem* **2013**, *6*, 1352–1356.
[20] L. Li, C. Stroobants, K. Lin, P. A. Jacobs, B. F. Sels, P. P. Pescarmona, *Green Chem.* **2011**, *13*, 1175–1181.
[21] J. Zhang, L. Wang, G. X. Wang, F. Chen, J. Zhu, C. T. Wang, C. Q. Bian, S. X. Pan, F.-S. Xiao, *ACS Sustainable Chem. Eng.* **2017**, *5*, 3123–3131.
[22] J. Pang, M. Zheng, X. Li, L. Song, R. Sun, J. Sebastian, A. Wang, J. Wang, X. Wang, T. Zhang, *Chem. Select* **2017**, *2*, 309–314.
[23] D. Padovan, S. Tolborg, L. Botti, E. Taarning, I. Sádaba, C. Hammond, *Reaction Chem. Eng.* **2018**, *3*, 155–163.
[24] E. Taarning, S. Saravanamurugan, M. S. Holm, J. Xiong, R. M. West, C. H. Christensen, *ChemSusChem* **2009**, *2*, 625–627.
[25] M. S. Holm, S. Saravanamurugan, E. Taarning, *Science* **2010**, *328*, 602–605.
[26] J. Wang, Y. Masui, M. Onaka, *Appl. Catal. B* **2011**, *107*, 135–139.
[27] H. Y. Luo, J. D. Lewis, Y. Román-Leshkov, *Annu. Rev. Chem. Biomol. Eng.* **2016**, *7*, 663–692.
[28] H. J. Cho, C. C. Chang, W. Fan, *Green Chem.* **2014**, *16*, 3428–3433.
[29] P. Y. Dapsens, C. Mondelli, J. Jagieski, R. Hauert, J. Pérez-Ramírez, *Catal. Sci. Technol.* **2014**, *4*, 2302–2311.
[30] J. Iglesias, J. Moreno, G. Morales, J. A. Melero, P. Juárez, M. López-Granados, R. Mariscal, I. Martínez-Salazar, *Green Chem.* **2019**, *21*, 5876–5885.
[31] L.-H. Chen, X.-Y. Li, G. Tian, Y. Li, J. C. Rooke, G.-S. Zhu, S.-L. Qiu, X.-Y. Yang, B.-L. Su, *Angew. Chem. Int. Ed.* **2015**, *54*, 10848–10851; *Angew. Chem.* **2015**, *127*, 10998–11001; *Angew. Chem.* **2015**, *127*, 10998–11001; *Angew. Chem. Int. Ed.* **2015**, *54*, 10848–10851.
[32] H. J. Cho, N. S. Gould, V. Vattipalli, S. Sabnis, W. Chaikittisilp, T. Okubo, B. Xu, W. Fan, *Microporous Mesoporous Mater.* **2019**, *278*, 387–396.
[33] Y. Sun, L. Shi, H. Wang, G. Miao, L. Kong, S. Li, U. Sun, *Sustainable Energy Fuels* **2019**, *3*, 1163–1171.

[34] W. Dong, Z. Shen, B. Peng, M. Gu, X. Zhou, B. Xiang, Y. Zhang, *Sci. Rep.* **2016**, *6*, 26713.

[35] X. Zhao, T. Wen, J. Zhang, J. Ye, Z. Ma, H. Yuan, X. Ye, Y. Wang, *RSC Adv.* **2017**, *7*, 21678–21685.

[36] P. Mäki-Arvela, I. L. Simakova, T. Salmi, D. Yu. Murzin, *Chem. Rev.* **2014**, *114*, 1909–1971.

[37] S. Van den Bosch, W. Schutyser, S. F. Koelewijn, T. Renders, C. M. Courtin, B. Sels, *Chem. Commun.* **2015**, *51*, 13158–13161.

[38] L. Penín, S. Peleteiro, V. Santos, J. L. Alonso, J. C. Parajó, *Cellulose* **2019**, *26*, 1125–1139.

[39] S. Xu, Y. Wu, J. Li, T. He, Y. Xiao, C. Zhou, C. Hu, *ACS Sustainable Chem. Eng.* **2020**, *8*, 4244–4255.

[40] M. J. Biddy, C. J. Scarlata, C. M. Kinchin, Chemicals from Biomass: A Market Assessment of Bioproducts With Near-Term Potential; NREL Report NREL/TP-5100-65509; National Renewable Energy Laboratory: Golden, CO, USA, **2016**. Global Lactic Acid Market Size, Market Share, Application Analysis, Regional Outlook, Growth Trends, Key Players, Competitive Strategies and Forecasts, 2015 to 2022 (accessed on 3.5 March 2020). https://www.nrel.gov/docs/fy16osti/65509.pdf.

[41] L. S. Sharninghausen, J. Campos, M. G. Manas, R. H. Crabtree, *Nat. Commun.* **2014**, *5*, 5084, 1–9.

[42] M. R. Arcanjo, I. J. Jr. Da Silva, C. L. Jr. Cavalcante, J. Iglesias, G. Morales, M. Paniagua, J. A. Melero, R. S. Vieira, *Biofuels Bioprod. Biorefin.* **2020**, *14*, 357–370.

[43] M. Dusselier, P. V. Wouwe, A. Dewaele, E. Makshina, B. F. Sels, *Energy Environ. Sci.* **2013**, *6*, 1415–1442.

[44] H. T. V. Lin, M. Y. Huang, T. Y. Kao, W. J. Lu, H. J. Lin, C. L. Pan, *Fermentation* **2020**, *6*, 37.

[45] X. Jin, J. Shen, W. Yan, M. Zhao, P. S. Thapa, B. Subramaniam, R. V. Chaudhari, *ACS Catal.* **2015**, *5*, 6545–6558.

[46] Y. Weng, S. Qiu, L. Ma, Q. Liu, M. Ding, Q. Zhang, T. Q. Zhang, T. Wang, *Catalysts* **2015**, *5*, 2147–2160.

[47] G. Li, E. A. Pidko, E. J. M. Hensen, *Catal. Sci. Technol.* **2014**, *4*, 2241–2250.

[48] J. C. Vega-Vila, J. W. Harris, R. Gounder, *J. Catal.* **2016**, *344*, 7025–7043.

[49] X. Zhu, L. Wu, P. C. M. M. Magustin, B. Mezari, E. J. M. Hensen, *J. Catal.* **2015**, *237*, 10–21.

[50] A. Corma, U. Diaz, V. Fornés, J. M. Guil, J. Martínez-Triguero, E. J. Creyghton, *J. Catal.* **2000**, *191*, 218–224..

[51] C. H. Tempelman, M. T. Portilla, M. E. Martinez-Armero, B Mezari, N. G. De Caluwé, C. Martínez, E. J. Hensen, *Microporous Mesoporous Mater.* **2016**, *220*, 28–38.

[52] S. Torborg, I. Sabada, C. M. Osmundsen, P. Fristrup, M. S. Holm, E. Taarning, *ChemSusChem* **2015**, *8*, 613–617.

[53] A. Corma, L. T. Nemeth, M. Renz, S. Valencia, *Nature* **2001**, *412*, 423–425.

[54] W. W. Graaff, G. Li, B. Mezari, E. A. Pidko, E. J. M. Hensen, *ChemCatChem* **2015**, *7*, 1152–1160..

[55] C. Hammond, S. Conrad, I. Hermans, *Angew. Chem. Int. Ed.* **2012**, *51*, 11736–11739; *Angew. Chem.* **2012**, *124*, 11906–11909; *Angew. Chem.* **2012**, *124*, 11906–11909; *Angew. Chem. Int. Ed.* **2012**, *51*, 11736–11739.

[56] A. Al-Nayili, K. Yakabi, C. Hammond, *J. Mater. Chem. A* **2016**, *4*, 1373–1382.

[57] T. H. Bae, J. R. Long, *Energy Environ. Sci.* **2013**, *6*, 3565–3569.

[58] A. R. Millward, O. M. Yaghi, *J. Am. Chem. Soc.* **2005**, *127*, 17998–17999.

[59] P. Wattanapaphawong, P. Reubroycharoen, A. Yamaguchi, *RSC Adv.* **2017**, *7*, 18561–18568.

[60] B. Arreguin, J. Taboada, *J. Chromatogr. Sci.* **1970**, *8*, 187–191.

[61] A. Parodi, E. Diguilio, S. Renzini, I. Magario, *Carbohydr. Res.* **2020**, *487*, 107885.

[62] S. Y. Chen, L. Y. Jang, C. Heng, *Chem. Mater* **2004**, *16*, 4174–4180.